REVIEWS

Journal of Semiconductors
(2020) 41, 091704
doi: 10.1088/1674-4926/41/9/091704

Recent progress in organic electrodes for zinc-ion batteries

Shuaifei Xu, Mingxuan Sun, Qian Wang, and Chengliang Wang†

School of Optical and Electronic Information, Wuhan National Laboratory for Optoelectronics (WNLO), Huazhong University of Science and Technology, Wuhan 430074, China

Abstract: Organic zinc-ion batteries (OZIBs) are emerging rechargeable energy storage devices and have attracted increasing attention as one of the promising alternatives of lithium-ion batteries, benefiting from the Zn metal (low cost, safety and small ionic size) and organic electrodes (flexibility, green and designable molecular structure). Organic electrodes have exhibited fine electrochemical performance in ZIBs, but the research is still in infancy and hampered by some issues. Hence, to provide insight into OZIBs, this review summarizes the progress of organic cathode materials for ZIBs and points out the existing challenges and then addresses potential solutions. It is hoped that this review can stimulate the researchers to further develop high-performance OZIBs.

Key words: organic electrodes; zinc-ion batteries; redox compounds

Citation: S F Xu, M X Sun, Q Wang, and C L Wang, Recent progress in organic electrodes for zinc-ion batteries[J]. *J. Semicond.*, 2020, 41(9), 091704. http://doi.org/10.1088/1674-4926/41/9/091704

1. Introduction

Lithium-ion batteries (LIBs) are one of the most successful commercial rechargeable energy storage devices with high energy density and long cycle life[1, 2]. However, they cannot satisfy the increasing energy demands, due to the scarcity of lithium resources and the potential safety concerns particularly when lithium metal is adopted as the anodes for the chase of high energy density (high reactivity with air and H_2O)[3, 4]. Zinc-ion batteries (ZIBs), a kind of emerging energy storage devices, are considered as one of the promising alternatives of LIBs. ZIBs contain a lot of advantages owing to the properties of Zn, including the higher abundance of Zn than Li (70 ppm for Zn vs. 20 ppm for Li in crust)[5], low cost, and small ionic radius (0.74 Å), etc.[6]. Moreover, due to the high safety of Zn metal (weak reactivity with air and H_2O), Zn metal is regarded as the most promising anode material for ZIBs, which shows high specific gravimetric capacity (820 mAh/g) and high specific volumetric capacity (5855 mAh/cm^3), although the cycling stability of ZIBs with Zn metal anode is also plagued by the possible formation of Zn dendrites. Fortunately, various methods have been proved to be effective to inhibit the growth of Li dendrites in Li-metal batteries[7–11], which could probably be also applicable to Zn metal for high cycleability[12–14]. In addition, Zn has proper electrode potential (0.76 V versus standard hydrogen electrode), making it possible to adopt an aqueous electrolyte, which has the merits of high ionic conductivity, low cost, green and nontoxicity.

Due to the possibility of using Zn metal as anodes, the study of cathode materials to match with the Zn anode is of the greatest interest for ZIBs[15–19]. Among the reported cathode materials for ZIBs, inorganic materials account for a large proportion, which consist of manganese-based oxides[20, 21], vanadium-based oxides[22, 23] and Prussian blue analogues[24, 25], etc. They have exhibited fairish Zn-storage performance. However, the development of inorganic cathode materials for ZIBs is hampered by some issues. For example, inorganic materials normally make use of toxic or environmental-unfriendliness transition metal elements. Besides, they suffer capacity fading due to the large volume change upon the insertion of Zn^{2+} ions[26, 27]. Compared to inorganic materials, organic materials are endowed with many advantages containing eco-friendliness, low-cost, lightweight, flexibility (small volume change during discharge–charge), designable molecular structure[28–31], which stimulate the exploration of organic cathode materials for ZIBs.

On the other hand, although aqueous electrolytes have a lot of advantages and most of the reported ZIBs adopted aqueous electrolytes, it should be noted that the aqueous electrolytes face the challenge of decomposition of water under larger electrochemical window, which would lead to poor cycleability of aqueous ZIBs (AZIBs). However, the organic cathode materials have the merits of tunable electrode potential through molecular design, which therefore are particularly suitable for aqueous ZIBs. To date, the reported ZIBs with organic cathodes are mostly based on aqueous electrolytes, and the relevant research progress is focused in this review. However, to comprehensively summarize the progress of organic cathodes for ZIBs, the investigation of organic ZIBs (OZIBs) based on non-aqueous electrolytes are also discussed (the mentioned electrolytes in this review are aqueous unless the solvent is specifically noted). The challenges and strategies to improve the performance of organic cathode materials are also addressed in each part. Finally, the perspectives on OZIBs are put forward in hope of developing high-performance ZIBs and energy storage devices.

2. Quinones

Quinones are a kind of representative organic electrode

Correspondence to: C L Wang, clwang@hust.edu.cn
Received 29 MAY 2020; Revised 14 JUNE 2020.

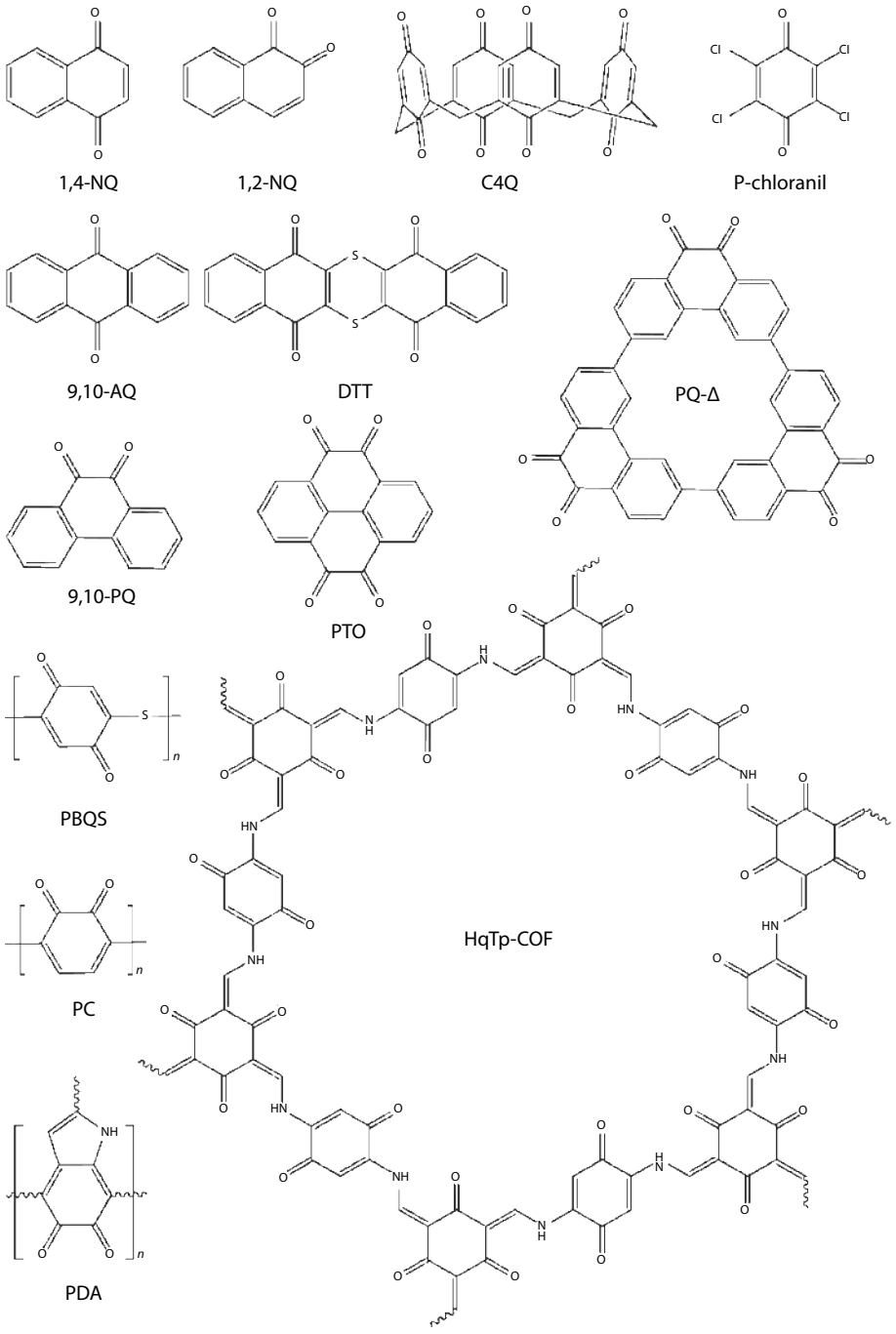

Fig. 1. The molecular structures of reported quinones as cathodes for ZIBs.

materials and have exhibited decent electrochemical performance (high capacity, high rate capability, long cycleability etc.) as cathodes in LIBs based on the stable redox reaction of carbonyls[32]. When the quinones accept electrons, the carbonyl groups (C=O) transform into enolates (C–O–Li). However, the investigation of quinones as cathodes for ZIBs is still in the primary stage (Fig. 1), and the energy storage mechanism is still under research. It is also considered as the transformation between C=O bonds and C–O bonds; however, because water is widely adopted as the solvent in the electrolytes of ZIBs, the intercalated counter ions might also be H^+ ions (in aqueous electrolytes) rather than Zn^{2+} ions[33]. To date, reported quinone-based cathodes for ZIBs can be classified into two types: insertion of Zn^{2+} ions and/or other cations.

2.1. Quinone-based cathodes with insertion of Zn^{2+} ions

Most quinones as cathodes for ZIBs are reported to bind with Zn^{2+} ions during discharge–charge process. A series of small molecular quinone-based cathodes for ZIBs exhibited decent Zn-storage performance (Fig. 2(a))[34]. Theoretical calculations (electrostatic potential (ESP) method) and experimental characterizations both manifested the carbonyl groups are the active sites for Zn^{2+} ion storage (Figs. 2(d) and 2(e)). Ortho-quinones (e.g. 1,2-naphthoquinone (1,2-NQ) and 9,10-phenanthrenequinone (9,10-PQ)) possess larger steric hindrance for ion insertion than that of para-quinones (e.g. 1,4-naphthoquinone (1,4-NQ), 9,10-anthraquinone (9,10-AQ)

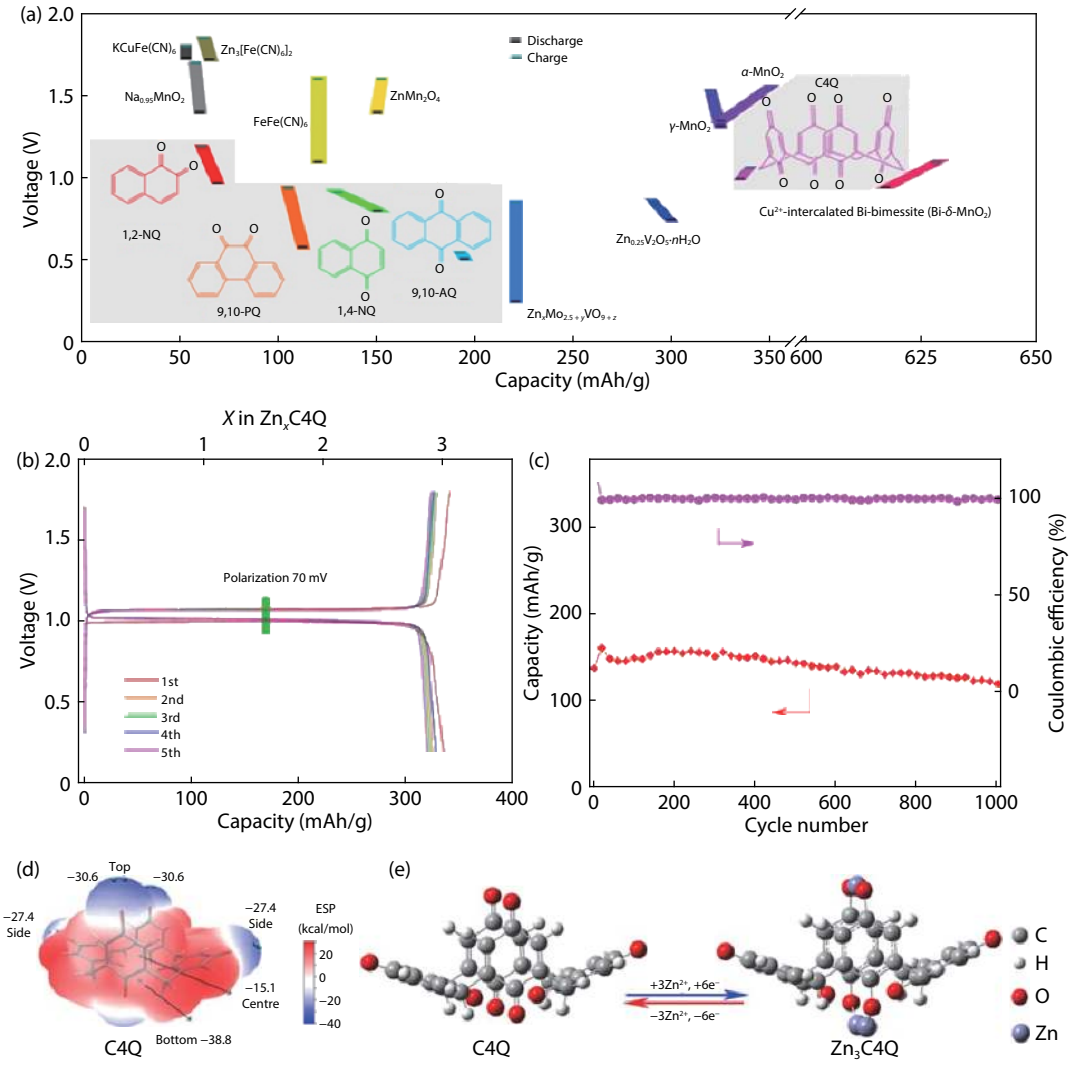

Fig. 2. (Color online) (a) The voltages and capacities of 1,2-NQ, 9,10-PQ, 1,4-AQ, 9,10-AQ and C4Q in ZIBs. (b) The charge-discharge profiles of C4Q at 0.02 A/g and (c) cycling performance at 0.5 A/g in ZIBs with a Nafion separator. (d) The ESP mapping of C4Q. (e) The optimized structure of the C4Q and Zn_3C4Q. Reproduced with permission from Ref. [34]. Copyright © 2018 American Association for the Advancement of Science.

and calix[4]quinone (C4Q)), resulting in lower capacity for ortho-quinones. However, all these small molecular quinones suffered capacity fading due to dissolution of discharged products (salts) in liquid aqueous electrolytes. With the aid of the Nafion membrane, the dissolution and the shuttle of the discharged salts were suppressed and the Zn anode was protected from being poisoned by discharged products. As a result, the C4Q-based cathode exhibited good cycling stability (Fig. 2(c), the capacity retention was 87% after 1000 cycles at 0.5 A/g) and high capacity (335 mAh/g at 0.02 A/g) with a small polarization voltage (Fig. 2(b), 70 mV).

As mentioned above, small molecular quinones usually suffered capacity decay due to the dissolution of discharged salts in aqueous electrolytes. However, it was reported that a pyrene-4,5,9,10-tetraone (PTO) cathode for AZIBs was inherently insoluble in aqueous electrolytes, as well as the discharged products, permitting high cycleability[35]. With normal glass fiber as the separator, the PTO cathode in a coin cell showed a high capacity of 336 mAh/g at 0.04 A/g and superior fast discharge-charge ability. Besides, a high capacity retention of 70% was achieved after 1000 cycles at 3 A/g. Notably, a flexible two-dimensinal (2D) belt shape Zn//PTO battery still delivered a comparable capacity (337 mAh/g at 0.04 A/g) with that in the coin cell. After bending at different angles, the battery still maintained the capacity well (Figs. 3(a) and 3(b)) and can power LEDs and fans (Fig. 3(c)), verifying its practicability.

It is accepted that polymers usually have low solubilities in electrolytes and hence are expected to exhibit decent cycleability[36–42]. However, it should be noted that the practical performance is highly dependent on the polymerization degree of the active materials and the low polymerization degree results in ineludible dissolution. For example, a poly(benzoquinonyl sulfide) (PBQS)-based cathode for AZIBs delivered a high initial capacity (203 mAh/g at 0.02 A/g); while the capacity loss was still observed, which may be due to its slight dissolution in aqueous electrolytes[36]. Compared to linear polymers, porous polymers are superior as electrode materials because the inherent porous structure can facilitate the infiltration of electrolytes and fast ionic transport, which contribute to high electrochemical performance[43–45]. For example, a HqTp covalent organic framework (COF), synthesized by poly-condensation of 2,5-diaminohydroquinone dihydrochloride (Hq) with 1,3,5-triformylphloroglucinol (Tp), possessed crys-

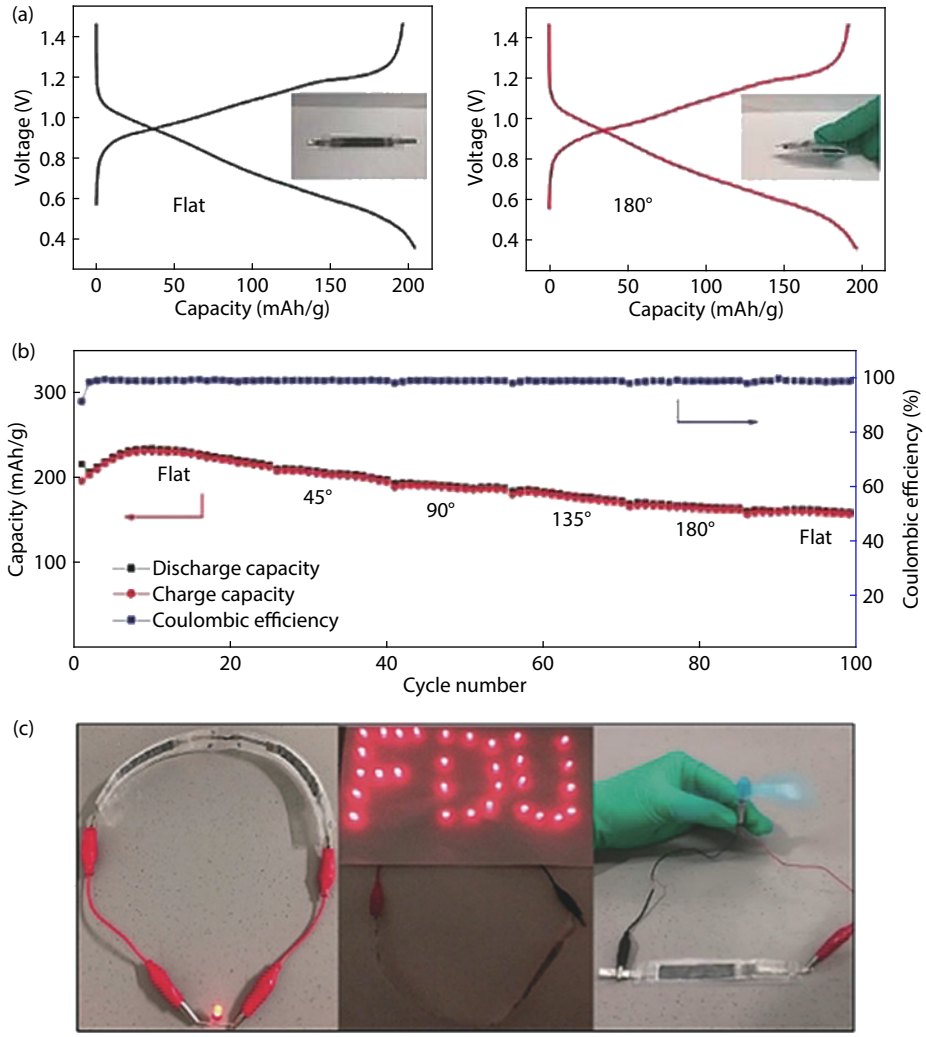

Fig. 3. (Color online) (a) The charge-discharge profiles of flexible Zn//PTO battery at flat state and 180° bending state at 1 A/g. (b) the cycling performance of flexible Zn//PTO battery at different bending state at 1 A/g. (c) the photos of LEDs and fan powered by the flexible Zn//PTO battery. Repoduced with permission from Ref. [35]. Copyright © 2018 WILEY-VCH Verlag GmbH & Co. KGaA, Weinheim.

talline porous structure with pore size of 1.5 nm[46]. The COF-based cathode exhibited a pair of redox peaks at 1.0/1.12 V vs. Zn/Zn^{2+} with a high capacity of 276 mAh/g at 0.125 A/g. Notably, with the Nafion membrane as the separator, the cycling performance was superior with a capacity retention of 95% after 1000 cycles at 0.15 A/g.

Thus, compositing polymers with conductive carbon materials is helpful for confining the polymers in the carbon materials and further inhibiting the dissolution of active materials. Moreover, the conductive carbon materials can increase the electrical conductivity of composite electrodes and thus benefits the rate capability[37, 38, 47, 48]. The composite of polydopamine (PDA) and carbon nanotubes (CNTs) showed high cycleability with capacity retention of 96% after 500 cycles at 0.2 A/g as a cathode for AZIBs (Fig. 4(c))[37]. The Zn-storage mechanism of PDA relied on the coordination of Zn^{2+} ions with the carbonyl groups (i.e. o-quinones) in PDA (Fig. 4(a)). The polycatechol (PC) electrode composited with graphene (Fig. 4(b)) (the active material content was ~23.3%) also exhibited better rate capability and cycleability (Fig. 4(d), 171 mAh/g at 10 C; retention of 74.4% after 3000 cycles at 2 C) (the active material content was ~23.3%) than the PC cathode (the active material content was 70%) (51 mAh/g at 10 C; retention of 62.2% after 2000 cycles at 2 C), which benefited from the high electrical conductivity and the confining effect of graphene, respectively[38]. However, the low active material content in the composite electrode would cause a low energy density of the whole battery. Both of PC and PDA exhibited Zn-storage performance based on the redox of carbonyl groups.

It was widely accepted that the volume change of flexible organic electrode materials is relatively small in comparison with inorganic materials[26, 49–52]. However, it was reported that the small volume change in organic electrode can still result in phase transition and lead to poor cycling performance. Experimental and density functional theory (DFT) calculations revealed the phase transition between tetrachloro-1,4-benzoquinone (p-chloranil) and Zn^{2+}-p-chloranil^{2-}, in which the molecular columns of p-chloranil rotated for accommodation of Zn^{2+} (Fig. 5(c))[51]. Though the volume change was small (~2.7%), the morphologies of p-chloranil cathodes changed significantly during cycling (Fig. 5(d)), leading to the detachment of active materials from the current collector and hence capacity fading (Fig. 5(a), the capacity retention was 34.15% after 30 cycles at 0.2 C). The appropriate conductive additives (CMK-3 carbon) can confine the p-chloranil from large

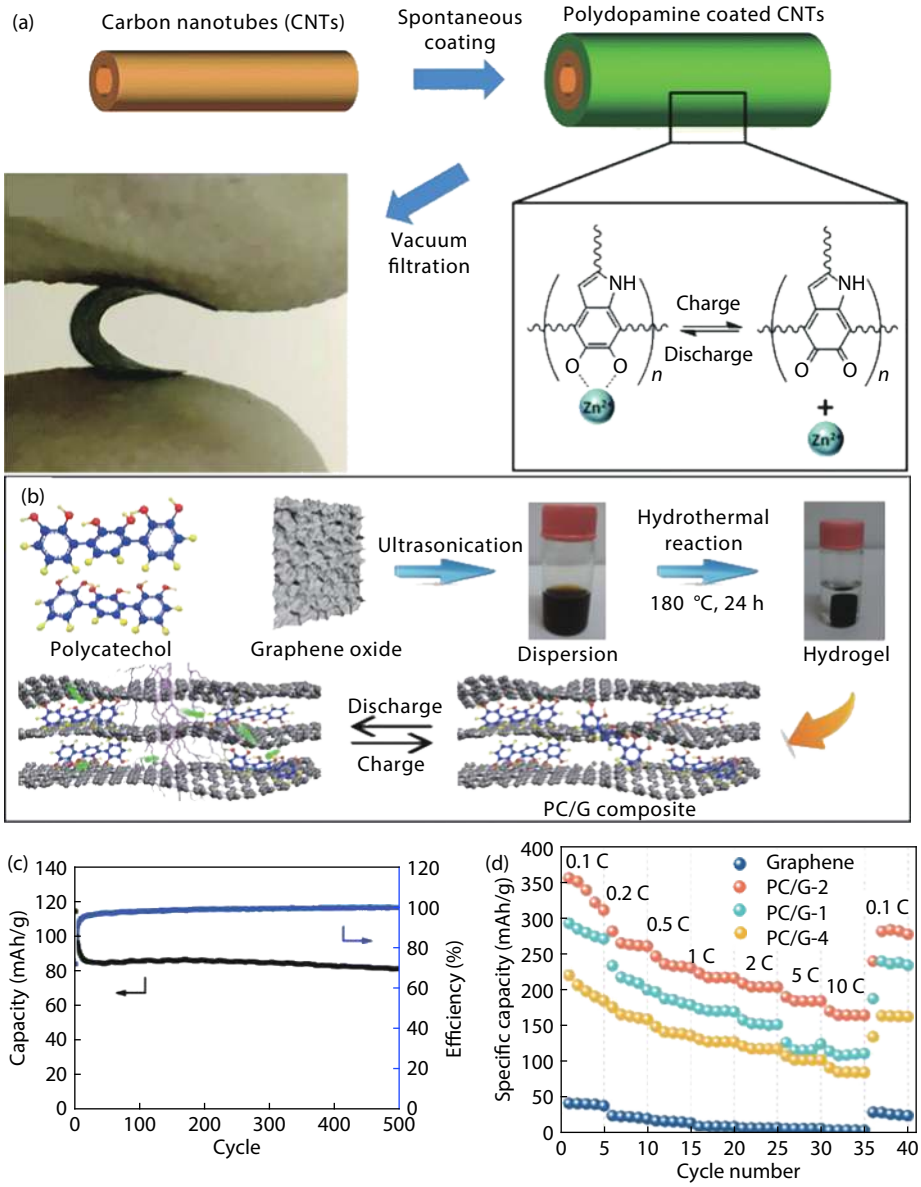

Fig. 4. (Color online) (a) The schematic diagram of the synthesis (top), photo (bottom left), and Zn-storage mechanism (bottom right) of PDA/CNTs. (b) The schematic diagram of the synthesis of PC/graphene. (c) Cycling performance of PDA/CNTs at 0.2 A/g in ZIBs. (d) Rate capability of PC/graphene. (a), (c) Reproduced with permission from Ref. [37]. Copyright © 2019 Royal Society of Chemistry. (b), (d) Reproduced with permission from Ref. [38]. Copyright © 2020 WILEY-VCH Verlag GmbH & Co. KGaA, Weinheim.

morphological variation (Fig. 5(e)), and thus the composite cathode exhibited a higher cycling performance (Fig. 5(b), the capacity retention was 70.34% after 200 cycles at 1 C)[51].

2.2. Quinone-based cathodes with insertion of more than Zn^{2+} ions

As mentioned above, most reported quinone-based cathodes for ZIBs are regarded to undergo the reversible coordination/de-coordination with Zn^{2+} ions during the discharge–charge process. However, some groups found that apart from Zn^{2+} ions, other ions in electrolytes can also bind with quinones and contribute capacity. Nam *et al.* believed that the discharge process of a triangular phenanthrenequinone-based macrocycle (PQ-Δ) was involved in the insertion of hydrated Zn^{2+} ions rather than the desolvated Zn^{2+} ions, which was revealed by the Fourier transform infrared spectroscopy (FTIR) and X-ray photoelectron spectroscopy (XPS) results (Figs. 6(a)–6(c))[53]. It was believed that the hydrated Zn^{2+} ions decreased the interfacial resistance between the electrolyte and cathode and hence was helpful for high Zn-storage performance, according to the DFT calculations that the co-insertion of H_2O molecules with Zn^{2+} ions lowered the desolvation energy. Moreover, benefiting from the robust triangular molecular structure of PQ-Δ, the inherent low solubility of the discharged/charged states in aqueous electrolytes endowed a long cycle life with high capacity (210 mAh/g and maintaining 99.9% after 500 cycles at 0.15 A/g). On the other hand, in an N, N-dimethylformamide (DMF) solution containing 0.5 M $Zn(CF_3SO_3)_2$, it is reported by another group that desolvated Zn^{2+} ions could coordinate with the carbonyl groups in PQ-Δ[54].

In view of the smaller size of H^+ ion than that of Zn^{2+} ion and the previous report that the MnO_2-based cathode for ZIBs displayed insertion of H^+ ions[55], it is reasonable to specu-

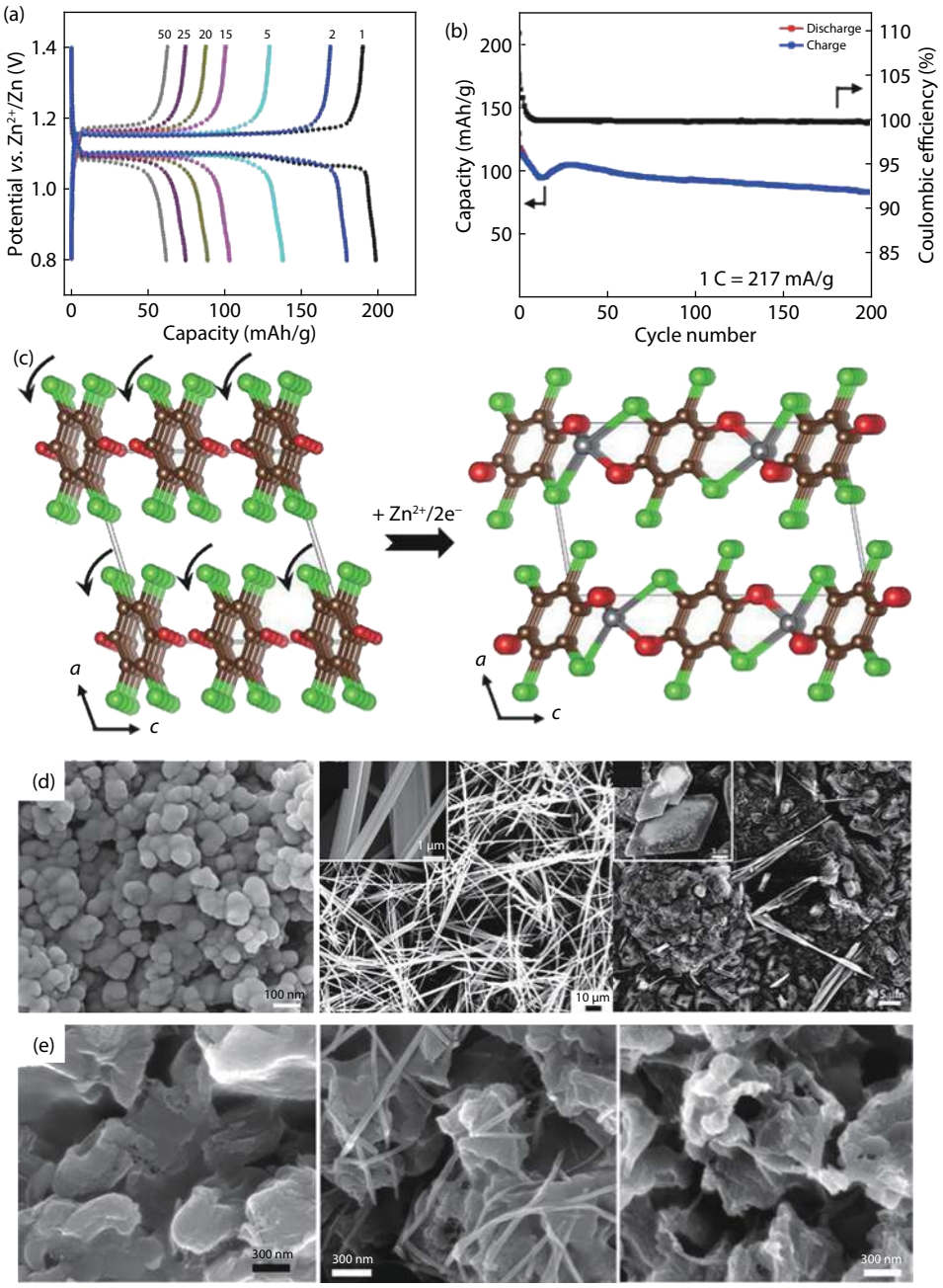

Fig. 5. (Color online) (a) The charge-discharge curves of p-chloranil at 0.2 C at different cycles. (b) The cycling performance of p-chloranil/CMK-3 at 1 C. (c) The calculated crystal structure of p-chloranil and Zn^{2+}-inserted p-chloranil; (d) SEM images of p-chloranil electrode and (e) p-chloranil/CMK-3 composite electrode at pristine (left), discharged (middle), and charged (right) state. Reproduced with permission from Ref. [51]. Copyright © 2018 American Chemical Society.

late that H^+ ions in aqueous electrolytes can also be inserted into organic electrodes for ZIBs with the co-insertion of Zn^{2+} ions. Such a phenomenon was discovered in a quinone-based cathode (sulfur heterocyclic quinone dibenzo[b,i]thianthrene-5,7,12,14-tetraone, DTT) for ZIBs recently[33]. The comparison of cyclic voltammetry (CV) tests of DTT in 1 M H_2SO_4 and 2 M $ZnSO_4$ (Fig. 6(d)) indicated that the DTT cathode in aqueous ZIBs can store H^+ ions and Zn^{2+} ions to form $DTT_2(H^+)_4(Zn^{2+})$. DFT calculations verified such mechanism. It was believed that one Zn^{2+} ion was coordinated with two carbonyls and four H^+ ions reacted with four carbonyls in two adjacent DTT molecules to form phenolic hydroxyls (the six-electron transfer for two DTT corresponded to a theoretical capacity of 213.8 mAh/g). Such stable structure of the discharged product benefited long-term cycleability. The DTT cathode exhibited high capacity (210.9 mAh/g at 0.05 A/g), fine rate capability (97 mAh/g at 2 A/g), and stable cycling performance (the capacity retention was 83.8% after 23 000 cycles at 2 A/g).

In a short summary, quinones exhibit fine Zn-storage performance with high capacity. However, it is worth noting that the research of quinone-based cathodes in ZIBs is in infancy, and they face some challenges. For instance, the dissolution behavior needs to be overcome by polymerization or compositing with carbon materials to achieve stable cycleability. Besides, the Zn-storage mechanism requires further investigation. And the redox voltages of quinones are relatively low, which restricts the energy density of ZIBs.

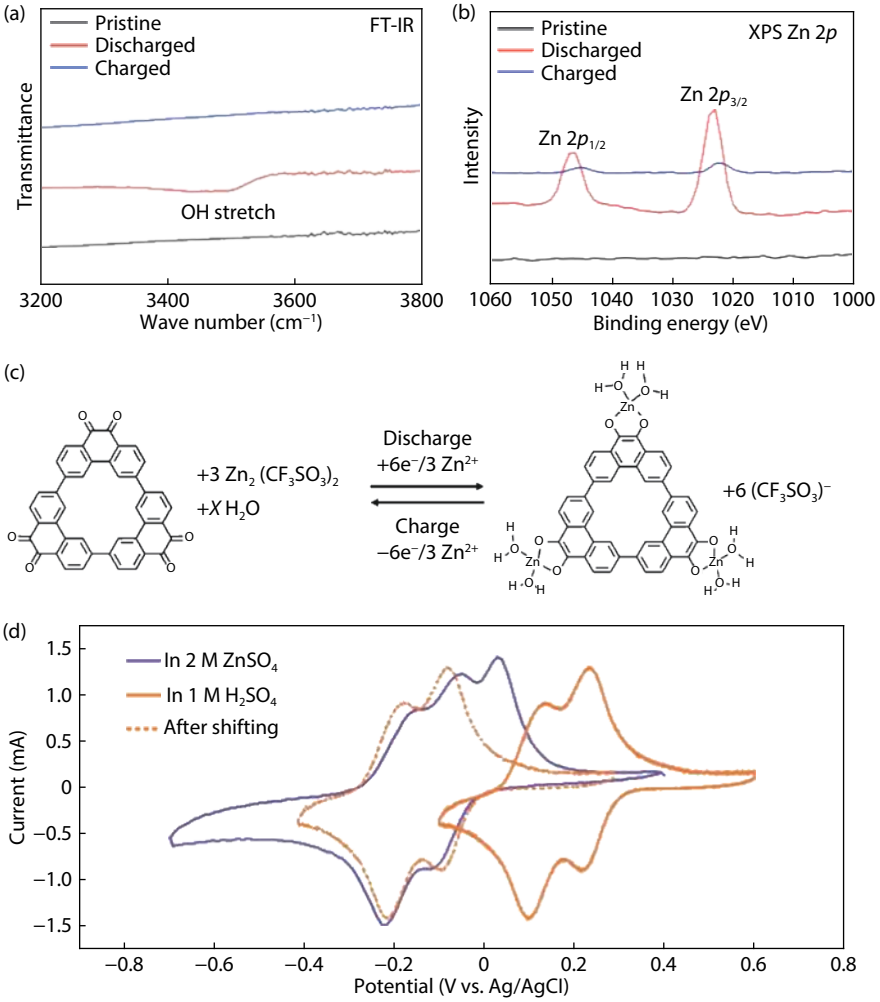

Fig. 6. (Color online) (a) The FTIR spectra and (b) XPS spectra of PQ-Δ at pristine, discharged and charged states. (c) The energy storage mechanism of PQ-Δ in 2 M $ZnSO_4$. Reproduced with permission from Ref. [53]. Copyright © 2020 American Chemical Society. (d) CV curves of DTT. Reproduced with permission from Ref. [33]. Copyright © 2020 WILEY-VCH Verlag GmbH & Co. KGaA, Weinheim.

3. Conducting polymers

Conducting polymers (CPs) are promising electrode materials for secondary batteries due to their high electrical conductivity and reversible redox reactions, which generally involve the anion-insertion in the polymer backbone. They have exhibited fine anion-storage performance as electrodes for metal-ion batteries[56, 57]. Compared to quinones, CPs exhibit higher redox voltage. Reported quinone-based cathodes for ZIBs all showed discharge voltages below 1 V, except p-chloranil (1.1 V)[51] due to the electron-withdrawing effect of –Cl groups. While PANI-based cathodes for ZIBs all exhibited discharge voltages above 1 V[58–60]. To date, reported CPs as cathodes for ZIBs include polyaniline (PANI), polypyrrole (PPy), polythiophene (PTh), poly(3,4-ethylenedioythiophene) (PEDOT), poly(p-phenylene) (PPP) and polyindole (PIn).

3.1. Polyaniline

Among various CPs, PANI is an attractive electrode material due to its fine redox reversibility, easy synthesis from chemical or electrochemical methods, and the stability in air. PANI has exhibited fine electrochemical performance in ZIBs, however, there are still some problems that restrict its further application.

It has been accepted that among three states (leucoemeraldine, pernigraniline, emeraldine) of PANI, the emeraldine form of PANI at the half-oxidized state can be doped (protonated) after acid doping and the resulting emeraldine salt possesses high electrical conductivity; while leucoemeraldine (fully reduced state) and pernigraniline (fully oxidized state) are insulators even when doped with acid (Fig. 7)[61, 62]. When charging, PANI can lose electrons, together with the acceptance of anions from the electrolytes; while reactions are reversed in the discharge process. Furthermore, it is believed that the protonation of PANI after acid doping is essential for electrochemical activity. However, the Zn anode suffers corrosion in acidic electrolytes. Therefore, it is important to select the pH value of electrolytes to balance the protection of Zn anode from corrosion (high pH value) and the high electrochemical activity of PANI (low pH value). To overcome such a problem and achieve high-performance PANI-based AZIBs, a lot of research has been done, mainly focusing on the modification of PANI.

3.1.1. Doped polyaniline

Forming doped PANI is the most common strategy for improving the electrochemical performance, which can be realized via chemical synthesis (called self-doped PANI) or forming composites with suitable materials that can provide protons. In this case, doped PANI can keep electrochemical activ-

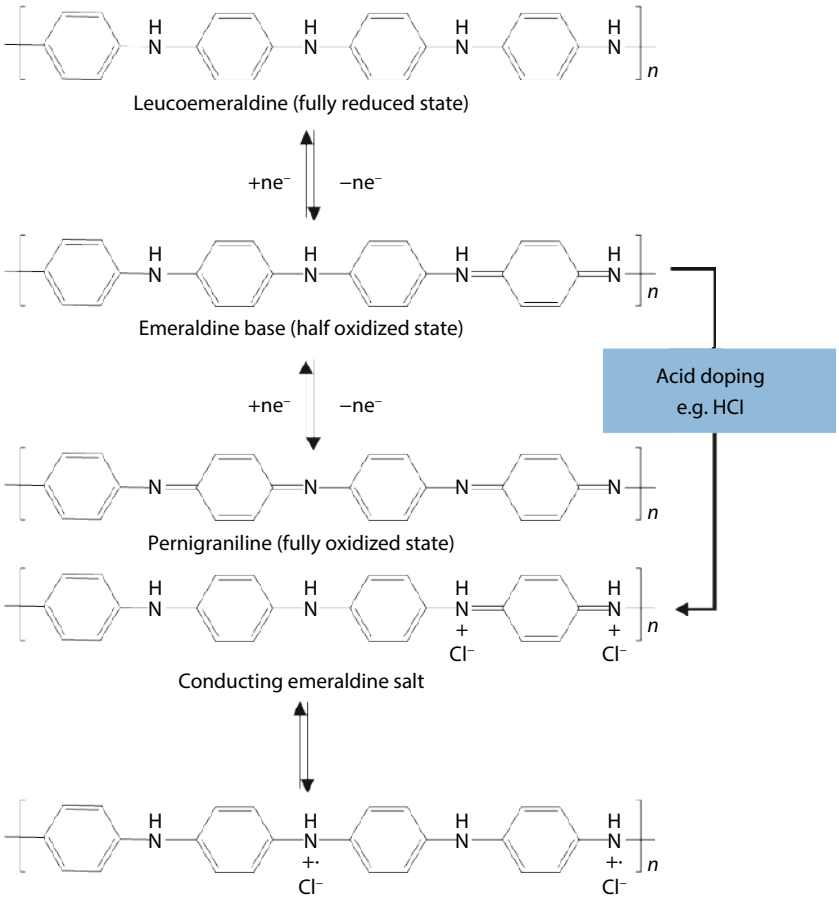

Fig. 7. The schematic diagram of the redox mechanism of PANI.

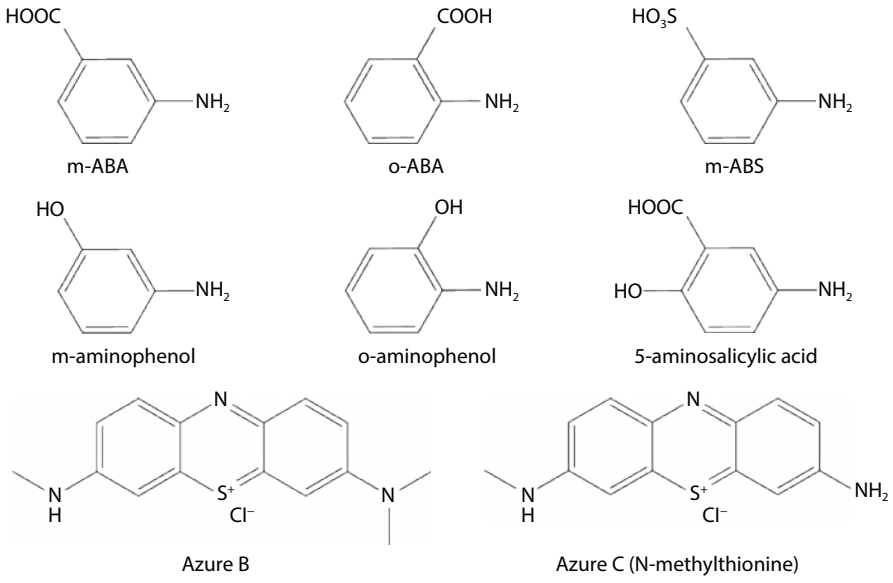

Fig. 8. Reported monomers for co-polymerization with aniline to form self-doped PANI.

ity in weakly acidic electrolytes, even neutral or basic electrolytes.

3.1.1.1. Self-doped polyaniline

It is an effective method to synthesize self-doped PANI by introducing substituent groups (as shown in Fig. 8, e.g., –COOH, –SO_3H, –OH, etc) as proton reservoirs.

For example, three aniline derivatives, o-aminobenzoic acid (o-ABA), m-aminobenzoic acid (m-ABA) and m-aminobenzenesulphonic acid (m-ABS) were employed to synthesize self-doped PANI via electro-polymerization with aniline[63, 64]. They all displayed redox activity in neutral electrolytes. Among them, PANI-co-m-ABS could keep electrochemical activity even in basic electrolytes with pH > 10. Shi *et al.* further proposed the reduction routes (Fig. 9(c)) of PANI-co-m-ABS (also called PANI-S)[65] according to the two reduction peaks in the differential capacity curves (Fig. 9(a)). The –SO_3H

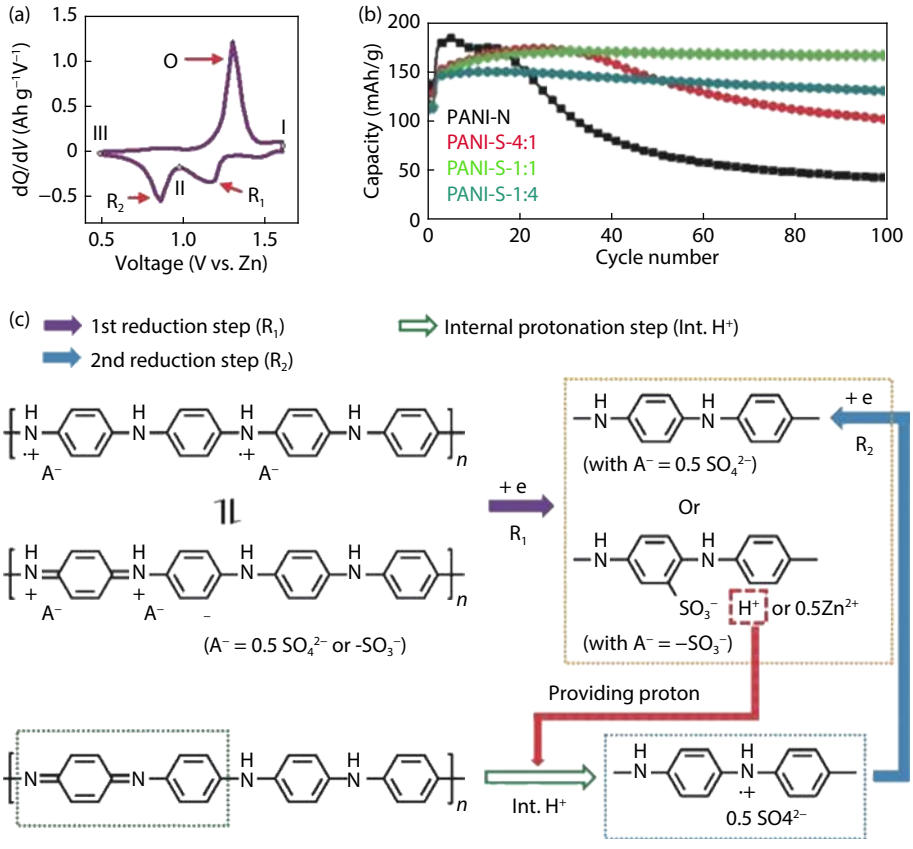

Fig. 9. (Color online) (a) The d*Q*/d*V* curve of PANI-co-m-ABS (also called as PANI-S) at 30th cycle. (b) The cycling performance of PANI-co-m-ABS and PANI at 1 A/g. (c) The redox pathways of PANI-co-m-ABS in 1 M $ZnSO_4$. Reproduced with permission from Ref. [65]. Copyright © 2019 WILEY-VCH Verlag GmbH & Co. KGaA, Weinheim.

group in the copolymer chain served as a proton reservoir because it could be ionized to $–SO_3^-$ in 1 M $ZnSO_4$ electrolyte, and thus provided a local acidic environment around the polymer without changing the overall pH value of the electrolyte, maintaining the electrochemical activity of PANI-co-m-ABS. Accordingly, the copolymer cathode exhibited superior performance with high rate capability (184 mAh/g at 0.2 A/g, 130 mAh/g at 10 A/g) and stable cycling performance (the capacity retention was 84.6% after 2000 cycles at 10 A/g), which outperformed PANI in the same electrolyte (Fig. 9(b)). Undoubtedly, by polymerizing aniline with 5-aminosalicylic acid, which contains both –OH group and –COOH group, the co-polymer, poly(aniline-co-5-aminosalicylic acid) (PANI-co-5-ASA), also exhibited good electrochemical activity in electrolytes with higher pH values[66].

It was reported that the meta-substituted ABA-based PANI derivatives showed higher electrochemical properties than the ortho-substituted counterparts[63]. Mu *et al.* applied two kinds of hydroxyl-substituted anilines (aminophenol) to co-polymerize with aniline to obtain PANI-co-o-aminophenol[67] and PANI-co-m-aminophenol[68], respectively, and utilized these two co-polymers as cathodes for AZIBs. The hydroxyls in the copolymer chain could not only tune the pH values around the cathodes, but also can undergo redox process. On account of this, the two co-polymers both exhibited higher capacity than PANI in the same electrolytes and could keep electrochemical activity in the electrolytes with higher pH values (> 4). Moreover, the meta-OH-substituted PANI derivative[68] showed better Zn-storage performance (137.5 mAh/g at 0.5 mA/cm^2; 94.5 mAh/g at 5 mA/cm^2) than its ortho-substituted analogue (103 mAh/g at 0.5 mA/cm^2; 64.7 mAh/g at 5 mA/cm^2)[67].

Apart from the co-polymerization of anilines with the substituted anilines, other redox-active monomers with proton-supply ability are also taken into consideration to synthesize self-doped PANI. PANMTh, which was synthesized by electrochemical copolymerization of aniline with N-methylthionine (also called as azure C), exhibited fine electrochemical activity in aqueous electrolytes with pH value of 10[69], which was attributed to the phenothiazine unit in N-methylthionine. The reversible redox of phenothiazine in neutral even basic aqueous electrolytes would undergo proton exchange between the electrode and the electrolytes, and thus endowed PANMTh with proton-self-supply ability, leading to its less dependence on the pH value of electrolytes. Moreover, higher capacity could also be expected due to the possible contribution from the phenothiazine. Consequently, this copolymer electrode for AZIBs showed high capacity (146.3 mAh/g at 1 mA/cm^2) and fine cycleability (the capacity retention was 99.4% after 150 cycles at 2 mA/cm^2)[70]. Another phenothiazine derivative, azure B, was also reported to form a copolymer with aniline. The resulting copolymer, poly(aniline-co-azure B) (PANAB), possessed good electrochemical activity at high pH values and exhibited enhanced performance with fine rate capability (127.8 mAh/g at 1 A/g)[71].

3.1.1.2. Mixing polyaniline with materials of proton-supply ability

In addition to the chemical synthesis, mixing PANI with

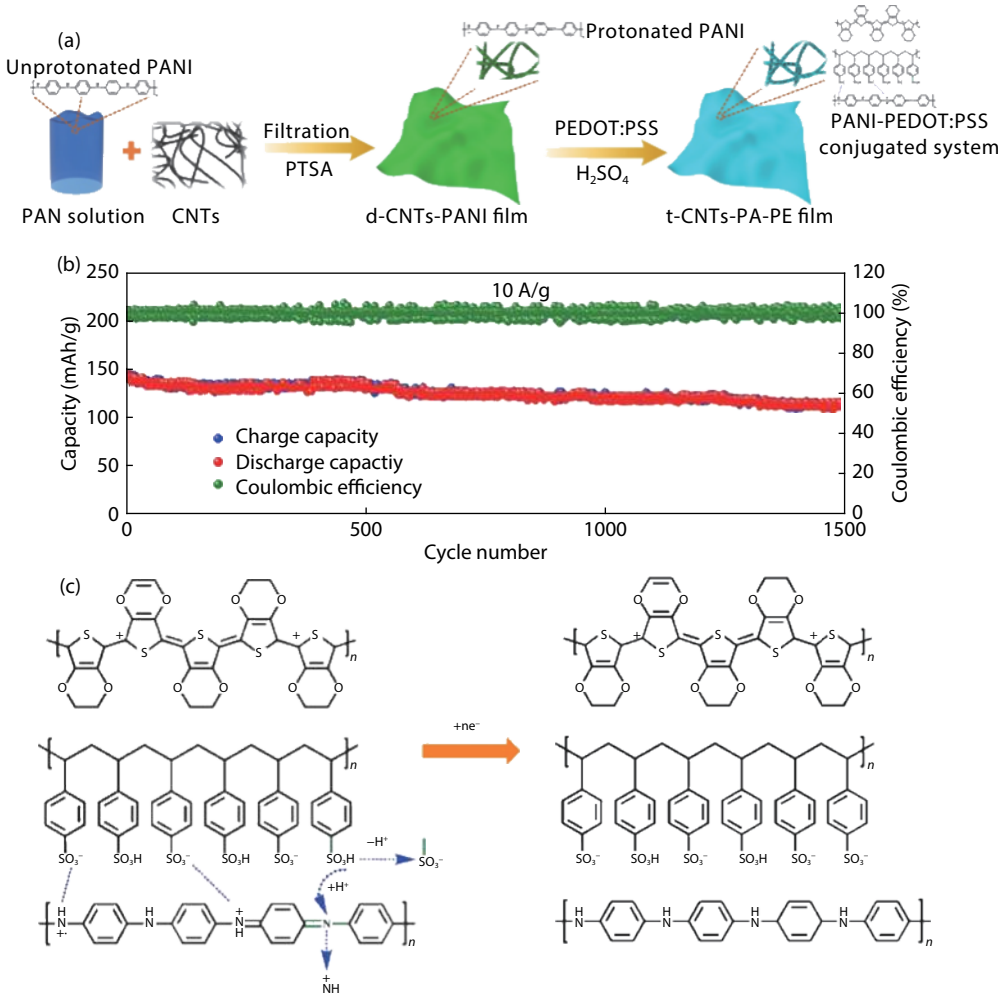

Fig. 10. (Color online) (a) The schematic diagram of the synthesis process, (b) long-term cycling performance at 10 A/g, and (c) proposed reduction mechanism of PANI-PEDOT:PSS-CNTs composite cathode in 2 M $ZnSO_4$. Reproduced with permission from Ref. [72]. Copyright © 2019 American Chemical Society.

materials that possess proton-supply ability is also effective to form the composite cathodes that are less dependent on the pH values of electrolytes. For example, poly(3,4-ethylenedioxythiophene) polystyrene sulfonate (PEDOT:PSS) is an electrically conductive polymer, where the $-SO_3H$ group in PSS can function as a proton reservoir and provide enough H^+ ions for the protonation of PANI (Fig. 10(c))[72]. The PANI cathodes mixed with PEDOT:PSS and carbon nanotubes (CNTs) (Fig. 10(a)) possessed enhanced electrical conductivity and proton-self-supply ability. Thus, superior rate capability (238 mAh/g at 0.2 A/g; 145 mAh/g at 10 A/g) and long cycle life (Fig. 10(b), the capacity retention was 77.9% after 1500 cycles at 10 A/g) were achieved. Besides PEDOT:PSS, graphene oxide (GO) was also favorable for the protonation of PANI, because the abundant hydroxyl groups of GO can serve as a proton reservoir[73, 74]. The PANI-GO composite electrodes exhibited higher capacity and cycling performance than those of PANI[73]. Compared to PANI-CNT, the PANI-GO composites with CNT as conductive additive also showed enhanced Zn-storage performance including capacity (233 mAh/g at 0.1 A/g; 100 mAh/g at 5 A/g) and cycling performance (the capacity retention was 78.7% after 2500 cycles at 3 A/g)[74].

The doping of PANI can also be achieved by using other materials. For example, after the electro-deposition of PANI on carbon cloth (CC), soaking them into aqueous solution of $K_3[Fe(CN)_6]$, and CC-PANI-FeCN composite was formed, where $[Fe(CN)_6]^{3-}$ ions were reduced to $[Fe(CN)_6]^{4-}$ ions by PANI during the soak process. Owing to the interactions between $-NH^+-/-NH^+=$ groups in PANI and $[Fe(CN)_6]^{4-}$ ions, the cycling performance of the CC-PANI-FeCN cathode (the capacity retention was 71% after 1000 cycles at 5 A/g) was superior to CC-PANI (capacity retention of 17% at same conditions) without the doping. Besides, fine rate capability (e.g. 162 and 125 mAh/g at 1 and 5 A/g, respectively) was achieved[75].

3.1.2. Compositing polyaniline with conductive materials

The above examples indicated that the electrochemical performance of PANI not only relies on its electrochemical activity, but also can be influenced by its electrical conductivity. In addition to the method by synthesizing doped PANI, another effective strategy for improving the electrical conductivity of PANI is mixing PANI with special conductive materials.

As one of the most efficient ways, PANI could be synthesized on the conductive materials during the electrochemical polymerization process, and thus the composite electrode with enhanced electrical conductivity can be directly used as electrodes for ZIBs. Different conductive substrates (Pt, carbon cloth (CC)[76], carbon rod[77], graphite[78], Ni foam[79]) have

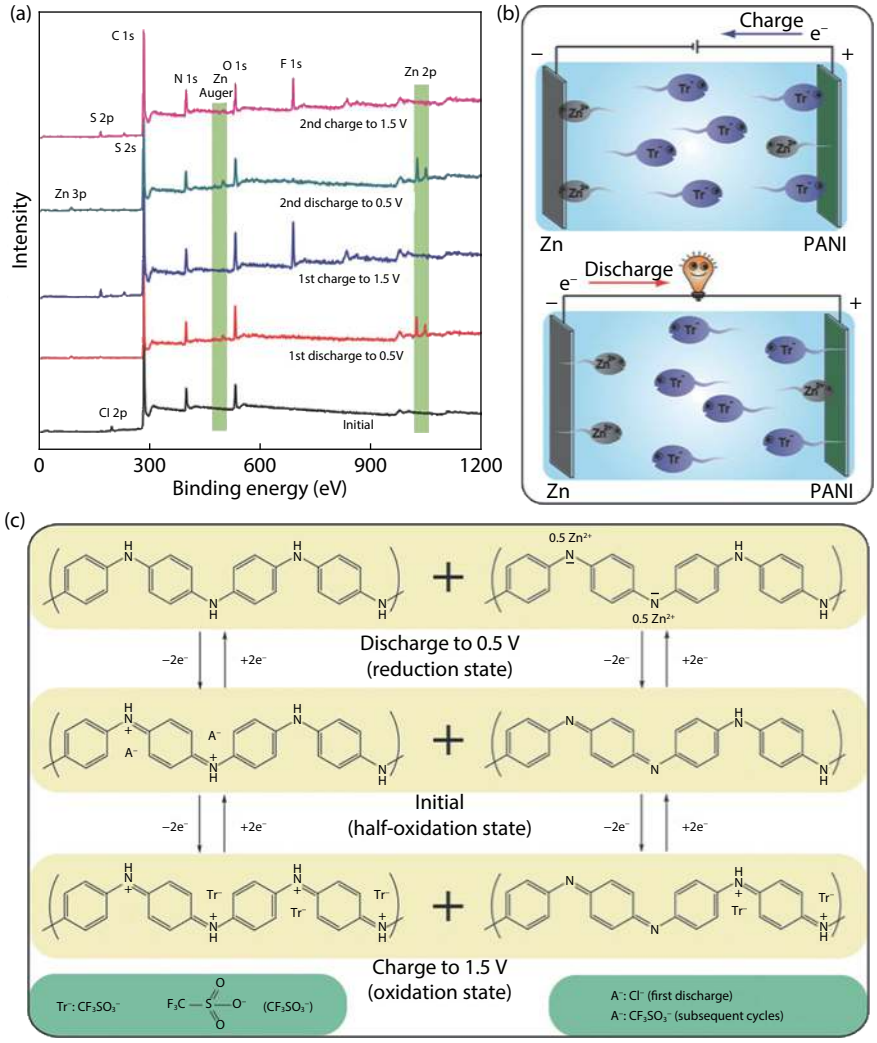

Fig. 11. (Color online) (a) Ex situ XPS spectra of PANI/CFs for ZIB at different state. (b) The schematic diagram of the ion storage mechanism of PANI/CFs. (c) The proposed redox mechanism of PANI/CFs in 1 M $Zn(CF_3SO_3)_2$. Reproduced with permission from Ref. [80]. Copyright © 2018 WILEY-VCH Verlag GmbH & Co. KGaA, Weinheim.

been adopted for the electro-polymerization of PANI. For example, the composites of PANI with graphite enhanced the electrical conductivity, facilitated the diffusion of dopant anions and increased the capacity[78]. Notably, compared to dense materials, porous conductive materials are superior as substrates because the resulted porous composite electrodes facilitate ionic transport. Li *et al.* achieved a 3D hierarchical electrode architecture via the electro-polymerization of PANAC on a CC-porous carbon scaffold[76]. The continuous porous conductive scaffold rendered fast ionic and electronic transport, and thus the CC-porous carbon@PANAC electrode showed higher capacity and rate capability than those of Pt plate@PANAC. In addition to carbon materials, other porous materials are also helpful for the fast reaction kinetics. With porous Ni foam as substrate, PANI[79] showed high rate capability (183.28 mAh/g at 2.5 mA/cm^2). Through in-situ chemical polymerization of PANI on carbon felts, the obtained PANI vertical nanostructure was favorable for the fast charge transfer[80]. The composite cathodes exhibited a high capacity of 200 mAh/g at 0.05 A/g with an average voltage of 1.1 V. Interestingly, energy dispersive X-ray spectroscopy (EDS) and ex situ XPS tests indicated that the Zn^{2+} ions and $CF_3SO_3^-$ ions both participated in the redox process of PANI using 1 M aqueous $Zn(CF_3SO_3)_2$ as electrolyte (Figs. 11(a) and 11(b)). Zn^{2+} ions can interact with –N= in half-oxidized PANI during discharge with the acceptance of electrons, while during charge process, the –NH– in half-oxidized PANI could transform to $=NH^+$-, along with the loss of electrons and interaction with $CF_3SO_3^-$ ions (Fig. 11(c)). High rate capability (95 mAh/g at 5 A/g) and superior cycling performance (the capacity retention was 92% after 3000 cycles at 5 A/g) were achieved. The high rate performance may be due to the surface-controlled electrochemical behavior.

Furthermore, it has been reported that the functionalization of carbon materials via pre-treatment or in situ process during polymerization of PANI is helpful to strengthen the interactions between carbon materials and PANI. For example, electron-cyclotron-resonance (ECR) plasma treatment is an effective method to oxidize the surface of carbon materials homogeneously. After the treatment of ECR O_2 plasma, the surface of carbon fibers (CF) had oxygen-containing functional groups (–OH, –COOH, –C=O). The functional groups enhanced the interactions with the deposited PANI, when such carbon fibers were used as substrates[81]. Besides, the surface of CF became rough, which increased the contact area between PANI and CF. Thus, the obtained composites (PANI-

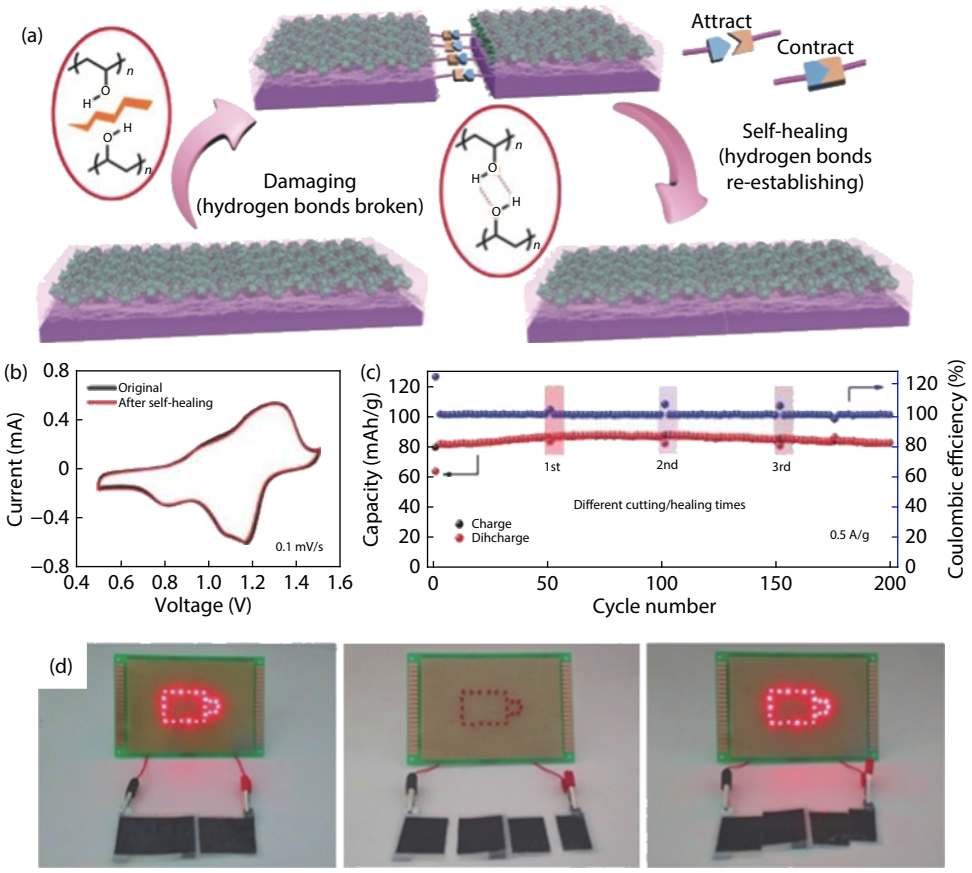

Fig. 12. (Color online) (a) The schematic diagram of the self-healing process of the all-in-one ZIB. (b) The CV curves of the original ZIB and the ZIB after self-healing. (c) The cycling performance of the ZIB after several self-healing. (d) The practical presentation of the self-healing ZIB. Reproduced with permission from Ref. [85]. Copyright © 2018 WILEY-VCH Verlag GmbH & Co. KGaA, Weinheim.

OCF) possessed higher structural robustness, leading to higher cycling performance than that of PANI-CF.

The aforementioned methods, including doping of PANI and mixing with conductive materials, are mainstream ways for improving the Zn-storage performance of PANI. Beyond these, the synthesis conditions of PANI, such as the control of monomer concentration[58, 82] or the ratio of different monomers for co-polymerization[63], also affected the electrochemical performance of PANI in AZIBs.

3.1.3. Polyaniline-based flexible Zn-ion batteries

In view of the fine Zn-storage performance of PANI and the rise of flexible electronics, flexible AZIBs based on PANI have attracted increasing attention based on gel polymer electrolytes (GPEs) recently. A sandwich-like flexible ZIB was fabricated with polyacrylamide (PAM)-$ZnSO_4$ GPE, nanowire array PANI cathode and nanosheet array Zn anode[82]. Benefiting from the nano-array electrode structure, shortened ionic diffusion length promoted the fast ionic transport, and thus facilitated high capacity and rate capability. Considering the non-interfering preparation of GPE and electrodes, all-in-one ZIBs could be made by integrating the GPE and electrodes. The GPEs are beneficial for improving the interfacial contact and thus contributing to durability under bending, twisting or compressing[82–84]. Zhang *et al.* fabricated an all-in-one PANI-based ZIB via a series of procedures[84], which included the spread of three kinds of suspensions in a Teflon mold (in the sequence of PANI/reduced graphene oxide (rGO) suspension, carbon nanofiber (CNF) suspension and Zn/exfoliated graphene (EG) suspension), freeze drying and subsequent injection of polyvinyl alcohol (PVA)-based GPE. Such all-in-one ZIB achieved tight contact between the electrode and electrolyte, and the continuous porous network benefited fast ionic and electronic transport, leading to good fast charge-discharge ability (79.5 mAh/g at 2 A/g) and stable cycling (the capacity retention was 94.6% after 500 cycles at 1 A/g). Owing to the abundant hydroxyl groups and corresponding hydrogen bonds in the PVA gel, the PVA-based GPEs fabricated via a facile freeze/thaw method possessed a self-healing function[85]. By integrating the cathode, anode and separator during the preparation of GPE, close contact and good interfacial stability were achieved between GPE and electrodes. After being broken and reconnected, the hydrogen bonds at the interface healed the function of the electrolyte and electrodes (Fig. 12(a)), and thus the ZIB could recover, which could even retain its original performance (Figs. 12(b)–12(d)). Impressively, Bi et al. found that the all-in-one PANI-based ZIBs possessed photo-detection ability when using transparent polyethylene terephthalate (PET) substrate[86]. Photocurrent could be detected under a white light with energy that was higher than the energy band of PANI. Such a novel bi-functional device broadens the application range of flexible electronic products.

In summary, PANI is validated to be a superior Zn-storage electrode material with fine performance. However, the electrochemical activity of PANI highly depends on the pH value of electrolytes, which should be acidic and hence help-

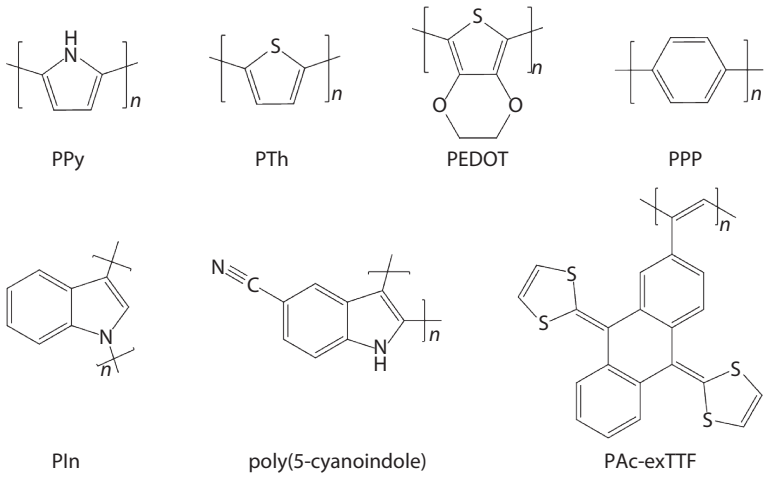

Fig. 13. The molecular structures of reported CPs as cathodes for ZIBs apart from PANI.

ful for the easy protonation. Unfortunately, under such circumstances, the Zn anode faces corrosion. Extensive efforts have been reported to solve this challenge and effective strategies include the doping of PANI by chemical synthesis or mixing with proper materials. Besides, the capacity of PANI is relatively low and limited by the doping level. Moreover, the energy storage mechanism of PANI in AZIBs needs further investigation. Recently, Zhao *et al.* reported a novel poly(1,5-naphthalenediamine, NAPD) cathode for ZIBs (the repeating unit was naphthalene for poly(1,5-NAPD) and benzene for PANI; both linkages are –NH– or =N–)[87]. The authors claimed that Zn^{2+} ions and H^+ ions both contributed to the capacity. Simultaneously, they also believed that SO_4^{2-} anions could be inserted into the poly(1,5-NAPD), which can be inferred by the one more reduction peak at high voltage in the $ZnSO_4$-based electrolyte than in the $Zn(CF_3SO_3)_2$-based electrolyte. The mechanism is different from the previous reports on PANI and probably needs further investigation.

3.2. Other conducting polymers

Apart from PANI, many other CPs (Fig. 13) have also demonstrated fine Zn-storage performance, such as polypyrrole (PPy)[88–93], polythiophene (PTh)[94], poly(3,4-ethylenedioythiophene) (PEDOT)[95, 96], polyindole (PIn)[97, 98] and poly(p-phenylene) (PPP)[99].

PPy is known as a bipolar CP, and both cations and anions could be inserted into PPy. Grgur *et al.* believed that the energy storage mechanism of PPy cathode for ZIBs was the insertion of anions from the electrolytes[93]. The PPy cathode exhibited similar capacity in 0.1 M HCl and 0.1 M NH_4Cl (pH = 5), which indicated the low dependence on pH values of the electrolytes. However, another group claimed a different mechanism by utilizing the p-toluenesulfonic anions (pTS^-) doped PPy as a cathode for ZIBs[91]. They claimed that due to the large size of anions, the energy storage mechanism of PPy/pTS^- relied on the cation exchange. During the reduction, the adsorption of cations balanced the pTS^- dopants; while during oxidization, the loss of electrons accompanied with the desorption of cations. The adsorption/desorption of cations can be monitored by the mass change of the electrodes. In this case, the 0.1 M NaCl electrolyte showed higher capacity than other electrolytes (0.1 M phosphate buffered saline (PBS), and 0.1 M simulated body fluid (SBS)), probably due to the smallest size of Cl^- anions in NaCl solution that had the weakest electro-static interaction with the cations in electrolytes. The weak interaction led to fast cation transport, which was favorable for high capacity. However, it was not clear if the mechanism was applicable to the electrolytes containing Zn^{2+} ions. Lahiri *et al.* investigated the Zn-storage performance of PPy in two kinds of electrolytes, of which the solutes were both $ZnAc_2$[92]. The difference was that one solvent was water and the other was a mixture solvent containing choline acetate (ChAc) and water. In situ Raman spectra indicated that the coordination of Zn^{2+} ions with PPy was responsible for the capacity. PPy cathode suffered capacity decay in both electrolytes due to the phase transition that was caused by the insertion of Zn^{2+} ions in the polymer cathode. Notably, the capacity of PPy in the electrolyte with water as the solvent was lower than that in the electrolyte with a mixed solvent. The result was attributed to the ChAc that reduced the strain during the insertion of Zn^{2+} ions.

Normally, the cycleability of PPy electrode was inferior[88] unless being composited with aerogel[90]. Wang *et al.* prepared PPy on a PET substrate by using electrodeposition (Fig. 14(a)) for flexible AZIBs, in which PVA-based GPE was the electrolyte. The transparent Zn//PPy AZIBs showed different colors at different charged/discharged voltages (as shown in Fig. 14(b): black for 1.2 V, yellow for 0 V) owing to the electro-chromic function of PPy[88]. Such unique property opened a door for the monitor of battery safety. However, PPy suffered severe capacity decay (the capacity retention was 38% after 200 cycles at 8.8 A/g). Accordingly, the electrochromic function of the PPy cathodes became weak after tens of cycles, which can be verified by the color of the battery at 0 V after different cycles (Fig. 14(c)). On the other hand, with the PVA-based aerogel as a scaffold, the PPy composite cathode showed better cycling stability (the capacity retention was 76.7% after 1000 cycles at 8 A/g) than the previous work, which may be due to the confining effect of the PVA-based aerogel to PPy[90]. Besides, benefiting from the porous structure of the scaffold and the nanofiber morphology of PPy, fast ionic transport was achieved in the PPy/aerogel, contributing to high rate capability (151.1 mAh/g at 0.5 A/g and 87.6 mAh/g at 16 A/g).

Similar to PANI and PPy, PIn is also a N-heterocyclic CP. It shows less dependence on the pH value of the electrolytes

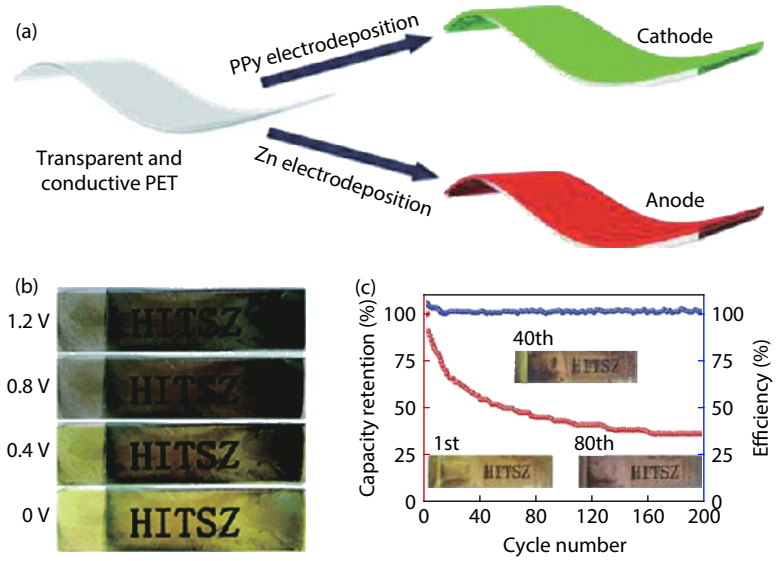

Fig. 14. (Color online) (a) The schematic diagram of the fabricating process of flexible Zn and PPy electrode on PET. (b) The color change of flexible Zn//PPy battery at different voltages. (c) The cycling performance of flexible Zn//PPy battery. Repoduced with permission from Ref. [88]. Copyright © 2018 Royal Society of Chemistry.

than PANI. In the 1990s, Pandey *et al.* reported PIn cathode for ZIB with 1 M $ZnSO_4$ electrolyte[97]. It delivered a maximum capacity of ~90 mAh/g in the voltage range from 0.75 to 1.45 V through a one-electron transfer process, and underwent reversible charge–discharge process for 50 cycles with CE close to 100%. Cai *et al.* also reported a Zn//PIn secondary battery with aqueous $ZnCl_2$ as electrolyte[98]. With the doping and dedoping of the Cl^- anions during the charge–discharge process, the voltage of the battery could reach 2 V and the PIn cathode delivered high rate capability (80 mAh/g at 0.02 mA/cm^2 and 60 mAh/g at 0.1 mA/cm^2). It also showed good cycleability with slow capacity fading (2.0% after 200 cycles) and thus small energy density decay (3.5% after 200 cycles). Besides, the PIn cathode exhibited high pH durability: the area of the CV curve in solutions with pH of 10 was 80.3% of that in solutions with pH of 6. Later, poly(5-cyanoindole) fibers via the electro-spinning technique were developed as the cathode for the ZIBs[100]. The battery achieved 2.0 V electromotive force and showed high rate performance with slow capacity decay (4% after 360 cycles at 0.2 C).

PTh, a S-heterocyclic CP, is also a potential cathode material for ZIB. The energy storage mechanism of PTh in ZIBs is considered as the doping/dedoping of anions from the electrolytes. The Zn//PTh battery showed an average discharge voltage of 1.2 V with 0.1 M $Zn(ClO_4)_2$ and 1 M $LiClO_4$ in propylene carbonate electrolyte and ClO_4^- anions could insert/extract into/from PTh reversibly during cycling[94]. However, the coulombic efficiency (CE) decreased with the increase of discharge rate (98% at 100 μA/cm^2; while 60% at 480 μA/cm^2). A PTh derivative, poly(3,4-ethylenedioythiophene) (PEDOT), as a cathode for ZIBs showed fine CE in 1-ethyl-3-methylimidazolium dicyanamide [C2mim][dca] ionic liquid (IL) electrolyte[95]. The high CE was ascribed to the inhibition of dendrite growth of metal anode in IL, although the PEDOT-based batteries still suffered capacity fading. Similar dendritic inhibition in IL was observed in Zn//PPP battery[99]. With polystyrene (PS) spheres assembled on the Zn sheets and the usage of IL as electrolytes, the growth of Zn dendrite was inhibited during cycling, which contributed to high cycleability (the capacity retention was over 90% after 300 cycles at 1 C) of the Zn//PPP battery. The PPP cathodes exhibited high redox voltage (discharge: 1.2 V; charge: 1.7 V); however, the low capacity (48 mAh/g at 0.2 C) would lead to a low energy density. Compared to IL, poly(ionic liquid) (PIL) iongel possesses similar physicochemical properties but without the risk of leakage. A solid-state Zn//PEDOT battery was fabricated with a PIL, i.e., poly (diallyldimethylammonium bis(trifluoromethanesulfonyl) imide) [p(DADMATFSI)] and 1-ethyl-3-methylimidazolium dicyanamide [emim][dca][96]. It showed a wide electrochemical window (–0.9 to 3.1 V vs. Zn/Zn^{2+}) and high ionic conductivity (1.1×10^{-2} S/cm at 50 °C).

Poly(acetylene) (PAc) is the first reported CP and its application as electrode materials for secondary batteries can date back to 1980s[101]. Häupler *et al.* reported a PAc-based polymer as cathodes for ZIBs, in which the side chain was 9,10-di(1,3-dithiol-2-ylidene)-9,10-dihydroanthracene (exTTF)[102]. The polymer cathode demonstrated a rapid charge–discharge ability and an improved electron transfer owing to the incorporation of redox-active moiety into the PAc backbone. Thus, high rate capability (100 mAh/g at 10 C; 47 mAh/g at 120 C) and good cycling performance were achieved in the voltage range of 0.6–1.7 V. However, the active material content in the electrode was low (50%), leading to low energy density.

In short, CPs are endowed with advantages of relatively high redox voltage as cathodes for ZIBs. Besides, fine rate capability could be expected owing to the high electrical conductivity; which, however, is affected by the doping level and the chemical environment (e.g. the pH value of the electrolytes). Furthermore, the capacity is also limited by the doping level. Thus, the modification of CPs needs further investigation for high-performance ZIBs.

4. Other redox compounds

In addition to the aforementioned organic/polymeric electrode materials, there are also many other redox-active organ-

ic materials that can be used as electrodes for ZIBs.

As representative carbonyl-based materials, quinones have been demonstrated as fine Zn-storage electrode materials and were studied widely. Other materials containing carbonyl groups were also reported. For example, anhydrides and imides are also potential cathode materials for ZIBs due to the redox activity of carbonyls. Wang *et al.* first reported 1,4,5,8-naphthalenetetracarboxylic dianhydride (NTCDA) and 1,4,5,8-naphthalene diimide (NTCDI) as cathodes for ZIBs[103]. NTCDA showed two pairs of redox peaks (discharge: 0.37, 0.58 V; charge: 0.54, 0.88 V) and suffered capacity fading. The peak at 0.37/0.54 V was identified to the insertion/extraction of hydronium in NTCDA. The poor cycling performance may be due to the structural damage upon the insertion of Zn^{2+} ions, which could be indicated by the new peak in the X-ray diffraction (XRD) pattern of the discharged NTCDA. NTCDI exhibited only one pair of redox peaks (discharge: 0.45 V; charge: 0.86 V), but higher capacity and rate capability (240 mAh/g at 0.1 A/g; 140 mAh/g at 2 A/g) than those of NTCDA (less than 180 mAh/g at 0.1 A/g and less than 20 mAh/g at 2 A/g). Besides, a better cycleability was achieved with a capacity retention of 73.7% after 2000 cycles at 1 A/g.

Apart from the carbonyl compounds, C=N groups containing materials are also expected to possess Zn-storage capacity due to the redox of C=N groups. For example, diquinoxalino [2,3-a:2′,3′-c] phenazine (HATN) and a HATN-based polymer have exhibited fine energy storage performance in LIBs[104], sodium-ion batteries, and potassium-ion batteries[105] and the active site was identified to the C=N groups, which could undergo reversible transformation to C-N group with the insertion of alkali metal-ions. Encouragingly, the Zn-storage performance of HATN is also superior with high capacity (370 mAh/g at 0.1 A/g; 123 mAh/g at 20 A/g) and good long-term cycleability (the capacity retention was 93.3% after 5000 cycles at 5 A/g)[106]. Such outstanding performance was ascribed to the unique H^+ coordination/de-coordination at C=N groups of HATN, which was revealed by ex situ spectra (FTIR, Raman, XPS) that the peaks of C=N disappeared while those of C–N and N–H enhanced during the discharge process. Fast kinetics of coordination/de-coordination of small H^+ ions and the π-conjugated structure of HATN benefited good rate capability, leading to high energy density of the battery.

In view of the variety of organic materials, a series of biomaterials with C=N and C=O groups, riboflavin (RF), alloxazine (ALX) and lumazine (LMZ), were reported as electrodes for ZIBs[107]. Among them, RF showed the lowest capacity (113.5 mAh/g at 0.03 A/g) but the highest cycling stability (the capacity retention was 92.7% after 5000 cycles at 5 A/g).

Organic materials containing C=O or/and C=N groups are both considered as cation-insertion electrode materials for ZIBs, and they have exhibited high capacity but the voltage is relatively lower than the anion-insertion electrode materials. In addition to conducting polymers, arylamine compounds can also be utilized as anion-insertion cathodes for ZIBs. For example, Glatz *et al.* reported a 1,4-bis(diphenylaminobenzene) (BDB) cathode for ZIBs in a high-concentrated electrolyte (19 M LiTFSI and 1 M $Zn(CF_3SO_3)_2$)[108]. The BDB cathode exhibited two pairs of redox peaks with a capacity of 112 mAh/g at 3 C (1 C = 0.13 A/g), corresponding to the insertion/extraction of two anions ($TFSI^-$ and $CF_3SO_3^-$) in each BDB molecule. The problem was that such a small molecular cathode material suffered capacity fading due to the dissolution of redox products in electrolytes. With a cellculose nanocrystal membrane as a protection layer on the cathode, fine cycling performance was achieved with a capacity retention of 82% after 500 cycles at 3 C. Besides, radical polymers are another kind of anion-insertion electrode materials and possess high redox voltage. Poly(2,2,6,6-tetramethylpiperidinyloxy-4-yl vinyl ether) (PTVE) cathode for ZIBs underwent a reversible one-electron redox process in aqueous electrolytes containing 0.1 M $ZnCl_2$ and 0.1 M NH_4Cl[109]. The PTVE cathode displayed a plateau voltage at 1.73 V (vs. Zn/Zn^{2+}) with discharge capacity of ~131 mA h/g at 60 C (~8 A/g) and could maintain 65% of the initial capacity after 500 cycles. In view of the anion-insertion mechanism of PTVE, it can be speculated that the anions may affect the electrochemical performance. Thus, Luo et al. further investigated the effects of three anions (SO_4^{2-}, $CF_3SO_3^-$, and ClO_4^-) on the electrochemical performance of the Zn//PTVE[110]. The PTVE cathode delivered capacities of 58, 52, and 50 mAh/g with average voltages of 1.77, 1.58, and 1.53 V at 10 A/g in 1 M $ZnSO_4$, $Zn(CF_3SO_3)_2$, and $Zn(ClO_4)_2$ electrolytes, respectively. The highest voltage in $ZnSO_4$ electrolyte was attributed to the highest binding energy between SO_4^{2-} anions with PTVE according to DFT calculations. Besides, a better cycleability (with a capacity retention of 77.0% after 1000 cycles at 1 A/g) was achieved in 1 M $Zn(CF_3SO_3)_2$ electrolyte than those in the other two electrolytes. Molecular electrostatic potential plots indicated that $CF_3SO_3^-$ anions possessed well-delocalized electronic structure, which was favorable for the dissociation from the PTVE host and thus contributed to the good cycling stability. However, it should be noted that the capacities in these electrolytes were much lower than the previous work in aqueous electrolyte containing 0.1 M $ZnCl_2$ and 0.1 M NH_4Cl, which may be due to the smaller ionic size of Cl^- anions and needs further investigation.

5. Conclusions and perspectives

The investigation of organic electrode materials for ZIBs is appealing due to the flexibility, eco-friendliness, and designable molecular structure of organic compounds. Organic electrode materials have exhibited fine Zn-storage performance (as shown in Table 1). However, the research of OZIBs is still in infancy and the further development is hampered by many issues. Aimed at these challenges, various strategies have been proved to be effective. The challenges and corresponding solutions are specifically summarized as follows:

(1) The dissolution behavior: Small molecular organic materials often suffer capacity decay due to the dissolution of discharged products in electrolytes. Fortunately, such an issue can be alleviated by many methods. Polymerization is the most effective way to inhibit the dissolution of small molecules. Applying functional separators[111, 112] (e.g. the Nafion membrane[34]) or compositing with carbon materials also helps. Besides, using solid electrolytes is another potential method, though they often face the challenges of low ionic conductivity and the reported solid-state ZIBs are mostly based on GPEs.

(2) The unclear energy storage mechanism: The Zn-stor-

Table 1. The performance of reported organic electrode materials for ZIBs. The abbreviations: Super P (SP), polytetrafluoroethylene (PTFE), poly(vinylidene fluoride) (PVDF), acetylene black (AB), carboxymethyl-cellulose (CMC), styrene-butadiene rubber (SBR), Ketjen black (KB), multi-walled carbon nanotubes (MWCNTs), single-walled carbon nanotubes (SWCNTs) and carbon black (CB).

Active material	Electrode composition (active material/ conductive additive/binder); conductive additive; binder	Electrolytes	Voltage range; discharge voltage (V) vs. Zn/Zn^{2+}	Capacity (mAh/g), current density (A/g)	Capacity retention (cycle number, current density (A/g))	Ref.
Quinone-based cathodes with insertion of Zn^{2+} ions						
AQ	5.6 : 3.4 : 1; SP; PTFE	2 M $ZnSO_4$	/	221.8, 0.8	44.9% (500, 0.8)	[113]
AQ	4.9 : 3.6 : 1.5; SP; PTFE	1 M $ZnSO_4$+0.05 M $MnSO_4$	0.1–1.2; 0.45	204.5, 0.2	84.3% (200, 0.2)	[114]
AQ	6 : 3.5 : 0.5; SP; PVDF	3 M $Zn(CF_3SO_3)_2$	0.25–1.75; 0.51	194, 0.02	/	[34]
1,2-NQ	6 : 3.5 : 0.5; SP; PVDF	3 M $Zn(CF_3SO_3)_2$	0.25–1.75	69, 0.02	/	[34]
1,4-NQ	6 : 3.5 : 0.5; SP; PVDF	3 M $Zn(CF_3SO_3)_2$	0.25–1.75	150, 0.02	/	[34]
9,10-PQ	6 : 3.5 : 0.5; SP; PVDF	3 M $Zn(CF_3SO_3)_2$	0.25–1.75	112, 0.02	/	[34]
C4Q	6 : 3.5 : 0.5; SP; PVDF	3 M $Zn(CF_3SO_3)_2$	0.25–1.75; 1.0	335, 0.05; 172, 1	87% (1000, 0.5)	[34]
PTO	6 : 3 : 1; KB; PTFE	2 M $ZnSO_4$	0.36–1.46; 0.63, 1.0	336, 0.04; 162, 5	70% (100, 3)	[35]
PBQS	6 : 3 : 1; conductive carbon; PVDF	3 M $Zn(CF_3SO_3)_2$	0.2–1.8; 0.95	203, 0.1C (0.02 A/g); 126, 5 C	86% (50, 0.2 C)	[36]
HqTp-COF	/	3 M $ZnSO_4$	0.2–1.6; 1.0	276, 0.125; 85, 3.75	95% (1000, 0.15)	[46]
PDA/CNTs (38/62)	/	3.3 M $ZnSO_4$	0.3–1.4; 0.91	126.2, 0.02; 43.2, 5	96% (500, 0.2)	[37]
PC	7 : 2 : 1; AB; PVDF	3 M $ZnSO_4$	0.2–1.9; 0.86	204, 0.1 C (0.05 A/g); 51, 10 C	62.2% (2000, 2 C)	[38]
PC/graphene (1/2)	7 : 2 : 1; AB; PVDF	3 M $ZnSO_4$	0.2–1.9	355, 0.1 C; 171, 10 C	74.4% (3000, 2 C)	[38]
p-chloranil	6 : 3.5 : 0.5; SP; CMC and SBR	1 M $Zn(CF_3SO_3)_2$	0.8–1.4; 1.1	205, 0.2 C	34.15% (30, 0.2 C)	[51]
p-chloranil	6 : 3.5 : 0.5; CMK-3; CMC and SBR	1 M $Zn(CF_3SO_3)_2$	0.8–1.4	170, 0.2 C; 118, 1 C	70.34% (200, 1 C)	[51]
Quinone-based cathodes with insertion of more than Zn^{2+} ions						
PQ-Δ	6 : 3 : 1; AB; PVDF	3 M $Zn(CF_3SO_3)_2$	0.25–1.6; 0.84	225, 0.03; 210, 0.15	99.9% (500, 0.15)	[53]
PQ-Δ	6 : 3 : 1; KB; PTFE	0.5 M $Zn(CF_3SO_3)_2$-DMF	0.1–1.7; 0.66	145, 0.05; 60, 50	negligible fading (20000, 1)	[54]
DTT	6 : 3 : 1; KB; PTFE	2 M $ZnSO_4$	0.3–1.4	210.9, 0.05; 97, 2	83.8% (23000, 2)	[33]
Conducting polymers : PANI						
PANI	/	1 M $ZnCl_2$+0.5 M NH_4Cl	0.8–1.7; 1.22	235.6, 0.31 mA/cm^2	67.5% (100, 0.31 mA/cm^2)	[58]
PANI	/	1 M $ZnCl_2$, pH~4	0.65–1.40; 1.05	151.5, 0.75 mA/cm^2; 64.625, 12 mA/cm^2	95.5% (30, 0.75 mA/cm^2)	[59]
PANI	7 : 2 : 1; SWCNT; PVDF	PVA-2 M $Zn(CF_3SO_3)_2$	0.5–1.5; 0.75, 1.05	123, 0.1; 94, 3	97.1% (1000, 1)	[85]
PANI	/	PVA-$Zn(CF_3SO_3)_2$	0.5–1.5; 0.73, 1.16	27.88 μAh/cm^2, 0.33 A/cm^3; 5.84 μAh/cm^2, 4 A/cm^3	56.7% (500, 0.66 A/cm^3)	[86]
PANI	8 : 1.5 : 0.5; CNT; PVDF	0.3 M $Zn(TFSI)_2$-propylene carbonate	0.3–1.6	148, 0.5 C; 70, 12 C	85% (2000, 1 C)	[115]
PANI	/	1 M $ZnSO_4$pH=4.6	0.75–1.35	108, /	/	[116]

Continued

Active material	Electrode composition (active material/ conductive additive/binder); conductive additive; binder	Electrolytes	Voltage range; discharge voltage (V) vs. Zn/Zn^{2+}	Capacity (mAh/g), current density (A/g)	Capacity retention (cycle number, current density (A/g))	Ref.
PANI	/	2 M $ZnCl_2$+3 M NH_4Cl	0.7–1.7	203.5, 0.5; 118.7, 16	Nearly unchanged (1000, 8)	[117]
Self-doped PANI						
PANI-co-m-ABA	/	1 M $ZnCl_2$+0.5 M NH_4Cl, pH=5	0.8–1.6	146.4, 1 mA/cm^2	~62% (200, 1 mA/cm^2)	[64]
PANI-co-m-ABS	/	1 M $ZnSO_4$	0.5–1.6	184, 0.2; 130, 10	84.6% (2000, 10)	[65]
PANI-co-5-ASA	/	0.50 M $ZnCl_2$ +1.5 M NH_4Cl, pH =4.8	0.75–1.65; 1.13	140.6, 1 mA/cm^2; 124.1, 5 mA/cm^2	/	[66]
PANI-co-o-aminophenol	/	2.5 M $ZnCl_2$+3 M NH_4Cl, pH=4.7	/	103, 0.5 mA/cm^2; 64.7, 5 mA/cm^2	/	[67]
PANI-co-m-aminophenol	/	2 M $ZnCl_2$+3 M NH_4Cl, pH=4.7	0.75–1.45; 1.05	137.5, 0.5 mA/cm^2; 94.5, 5 mA/cm^2	/	[68]
PANMTh	/	2 M $ZnCl_2$+3 M NH_4Cl	0.7–1.5	146.3, 1 mA/cm^2	99.4% (150, 2 mA/cm^2)	[70]
PANAB	/	2 M $ZnCl_2$+3 M NH_4Cl, pH=4.7	0.7–1.5; 1.08	134, 0.12; 127.8, 1	61.4% (181, 0.2)	[71]
PANAC(PANMTh)	/	2 M $ZnCl_2$+3 M NH_4Cl, pH=5	0.7–1.5; 1.15	306.3, 0.28; 82.6, 3.92	73% (1100, 0.532)	[76]
PANAC	/	PVA-$ZnCl_2$-NH_4Cl	0.7–1.5	241.4, 0.22; 81.2, 1.33	68% (1000, 0.532)	[76]
PANFc	/	2.5 $ZnCl_2$+3 M NH_4Cl, pH=4.4	0.7–1.4; 1.0	124, 0.035	/	[118]
Mixing polyaniline with materials of proton-supply ability						
CNTs-PANI-PEDOT:PSS	/	2 M $ZnSO_4$	0.5–1.6; 0.72, 1.14	238, 0.2; 145, 10	77.9% (1500, 10)	[72]
CNTs-PANI-PEDOT:PSS	/	PAM-$ZnSO_4$	0.5–1.6; 0.72, 1.13	208, 0.2; 124, 5	/	[72]
PANI/GO	/	1.5 M $Zn(ClO_4)_2$+0.5 M NH_4ClO_4	0.7–1.55	183, 0.2 C; 147.8, 1 C	89.4% (100, 0.2 C)	[73]
CC-PANI-FeCN	/	1 M $ZnSO_4$	0.5–1.6	162, 1; 125, 5	71% (1000, 5)	[75]
Compositing PANI with conductive materials						
PANI-GO/CNT	/	2 M $Zn(CF_3SO_3)_2$ with 5 vol% diethyl ether	0.5–1.6	233, 0.1; 100, 5	78.7% (2500, 3)	[74]
PANI/porous carbon rod	/	1 M $ZnCl_2$+0.5 M NH_4Cl+3.7×10^{-4} M $HgCl_2$	1.12	/	~90% (100, /)	[77]
PANI/graphite	/	1 M $ZnCl_2$+0.5 M NH_4Cl, pH=4	0.7–1.7	142.4, 0.6 mA/cm^2	57.4% (200, 0.6 mA/cm^2)	[78]
PANI/Ni foam	/	1 M $ZnSO_4$ + 0.3 M $(NH_4)_2SO_4$	0.7–1.6	183.28, 2.5 mA/cm^2	/	[79]
PANI/carbon felts	/	1 M $Zn(CF_3SO_3)_2$	0.5–1.5; 0.65, 0.85, 1.07	200, 0.05; 95, 5	92% (3000, 5)	[80]
PANI/carbon felts	/	PVA-$Zn(CF_3SO_3)_2$	0.5–1.5	109, 5	/	[80]
PANI/OCF	/	PVA-1 M $ZnCl_2$+0.5 M NH_4Cl	0.7–1.5	104.67, 0.1; 83.8, 2	95.4% (200, 0.1)	[81]

Continued

Active material	Electrode composition (active material/ conductive additive/binder); conductive additive; binder	Electrolytes	Voltage range; discharge voltage (V) vs. Zn/Zn^{2+}	Capacity (mAh/g), current density (A/g)	Capacity retention (cycle number, current density (A/g))	Ref.
PANI/CNT	/	PAAM-1 M $ZnSO_4$	0.3–1.6; 1.1	144, 0.2; 90, 1	91.1% (150, 0.5)	[82]
PANI-SWCNT	/	PVA-$Zn(CF_3SO_3)_2$	0.5–1.5	212, 0.1; 68, 2	90.7% (1000, 1)	[83]
PANI/rGO	/	CNF/PVA-$Zn(CF_3SO_3)_2$	0.5–1.5	175.5, 0.1; 79.5, 2	94.6% (500, 1)	[84]
PANI/graphite/AB (80 : 18 : 2)	/	2 M $Zn(ClO_4)_2$ +1 M NH_4ClO_4 + 3.7×10^{-4} M Triton-X100 pH=3	/	125.4, 0.05	94.1% (100, 0.05)	[119]
		Other conducting polymers				
PPy	/	2 M $ZnAc_2$ in ChAc + 70% H_2O	0–1.5; 0.55	160, 0.5	43.75% (50, 0.5)	[92]
PPy	/	PVA-KCl-$ZnAc_2$	0–1.2	123, 1.9	38% (200, 8.8)	[88]
PPy/aerogel	/	Cellulose-2 M $ZnCl_2$ + 3 M NH_4Cl	0.6–1.6	151.1, 0.5; 87.6, 16	76.7% (1000, 8)	[90]
PTh	/	0.1 M $Zn(ClO_4)_2$ + 1 M $LiClO_4$-propylene carbonate	0.2–1.7; 1.2	/	/	[94]
PEDOT	8.5 : 1 : 0.5; SP; PVDF	[C2mim][dca] + 3 wt% water + $Zn(dca)_2$	0.5–1.6	28.5, 0.0075; 25.5, 0.075	66.7% (100, /)	[95]
PEDOT	/	65% p(DADMATFSI)- 35% $Zn(dca)_2$/[emim][dca]) + water + Al_2O_3	0.5–1.6	51, 0.01 mA/cm^2; 31, 0.02 mA/cm^2	/	[96]
PPP	8 : 1.2 : 0.8; amorphous carbon + graphite; PVDF	0.2 M $Zn(TfO)_2$/[EMIm]TfO-PS composite	0.3–1.8	48, 0.2 C	90% (300, 1 C)	[99]
PIn	/	1 M $ZnSO_4$	0.75–1.45	90, 20 μA/cm^2	/	[97]
PIn	6 : 3 : 1; CB; PTFE	$ZnCl_2$	1.0–2.0	81, 200 A/m^2; 60, 1000 A/m^2	98% (200, 500 A/m^2)	[98]
Poly(5-cyanoindole)	/	1 M $ZnCl_2$	1.0–2.2	107, 0.2 C; 61, 10 C	96% (360, 0.2 C)	[100]
PAc-exTTF	5 : 5 : /; MWCNT; /	1 M $Zn(BF_4)_2$	0.6–1.7; 1.1	100, 10 C; 47, 120 C	81% (10000, 10 C)	[102]
		Other redox compounds				
NTCDA	/	2 M $ZnSO_4$	0.37, 0.58	/	/	[103]
NTCDI	/	2 M $ZnSO_4$	0.45	240, 0.1; 140, 2	73.7% (2000, 1)	[103]
HATN	6 : 3.5 : 0.5; SP; PVDF	2 M $ZnSO_4$	0.3–1.1	370, 0.1; 123, 20	93.3% (5000, 5)	[106]
RF	6 : 3.5 : 0.5; CB; PVDF	3 M $Zn(CF_3SO_3)_2$	0.2–1.4; 0.6	113.5, 0.03; 95.8, 5	92.7% (5000, 5)	[107]
ALX	6 : 3.5 : 0.5; CB; PVDF	3 M $Zn(CF_3SO_3)_2$	0.2–1.4; 0.56	230.5, 0.05	62.13% (50, 0.05)	[107]
LMZ	6 : 3.5 : 0.5; CB; PVDF	3 M $Zn(CF_3SO_3)_2$	0.2–1.4; 0.47	252.8, 0.05	54.53% (50, 0.05)	[107]
BDB	6 : 3.5 : 0.5; SP; CMC/SBR (2/1)	19 M LiTFSI+1 M $Zn(CF_3SO_3)_2$	0.6–1.8; 0.89, 1.27	112, 3 C	82% (500, 3C)	[108]
Poly(1,5-NAPD)/AC	/	2 M $ZnSO_4$	0.1–1.8	315, 0.191; 145, 14.5	91% (10000, 10)	[87]
PTVE	5 : 4 : 1; SP; PVDF	1 M $ZnSO_4$	1.30–1.95; 1.70	58, 10	21.9% (1000, 1 A/g)	[110]
PTVE	5 : 4 : 1; SP; PVDF	1 M $Zn(ClO_4)_2$	1.30–1.95; 1.44	50, 10	/	[110]
PTVE	5 : 4 : 1; SP; PVDF	1 M $Zn(CF_3SO_3)_2$	1.30–1.95; 1.53	52, 10	77.0% (1000, 1 A/g)	[110]
PTVE/glassy carbon	/	0.1 M $ZnCl_2$+0.1 M NH_4Cl	1.4–2.0; 1.73	131, 60 C (~8 A/g)	65% (500, 60 C)	[109]

age mechanism is essential for further enhancing the performance OZIBs (particularly in aqueous electrolytes due to the various ions) and needs further exploration. For example, the Zn-storage mechanism of carbonyl compounds is considered as the coordination of Zn^{2+} ions with carbonyls, but some reports showed that quinones could also bind with H^+ ions (e.g. DTT) or hydrated Zn^{2+} ions (e.g. PQ-Δ) during discharge.

(3) Inherent restrictions resulting from the organic electrode materials: Various organic materials have been validated to be promising cathodes for ZIBs and they have exhibited fine performance. However, they often suffer their own shortcomings. For example, quinones possess high capacity due to the abundant Zn-storage active sites, but the redox voltage is not high. The potential could be elevated to a certain extent, by introducing electron-withdrawing groups. Furthermore, the low electrical conductivity of quinones restricts their rate capability. It seems that the CPs with high electrical conductivity and high voltage are more promising as cathodes for ZIBs. But the capacity of CPs is low. Particularly, the acidic electrolytes are necessary to guarantee the electrochemical activity of PANI, but such electrolytes would cause Zn corrosion.

(4) The universal problems in ZIB, such as the low electrochemical window of aqueous electrolytes, the corrosion of Zn metal and the possible growth of Zn dendrites, are out of the scope of this review and will not be further illustrated here.

In conclusion, rapid development of OZIBs is expected if the above challenges can be solved well. We hope this review can provide insight into the development of high performance OZIBs.

Acknowledgements

This work was supported by the National Natural Science Foundation of China (No. 51773071), the National 1000-Talents Program, Innovation Fund of WNLO and the Fundamental Research Funds for the Central Universities (HUST : 2017KFYXJJ023, 2017KFXKJC002, 2018KFYXKJC018, and 2019kfyRCPY099).

References

[1] Armand M, Tarascon J M. Building better batteries. Nature, 2008, 451, 652
[2] Dunn B, Kamath H, Tarascon J M. Electrical energy storage for the grid: A battery of choices. Science, 2011, 334, 928
[3] Hwang J Y, Myung S T, Sun Y K. Sodium-ion batteries: Present and future. Chem Soc Rev, 2017, 46, 3529
[4] Hosaka T, Kubota K, Hameed A S, et al. Research development on K-ion batteries. Chem Rev, 2020, 120, 6358
[5] Allegre C, Michard G. Introduction to geochemistry. Boston: D. Reidel, Dordrecht-Holland, 1983
[6] Marcus Y. Ionic radii in aqueous solutions. Chem Rev, 1988, 88, 1475
[7] Wang B, Wu Y C, Zhuo S M, et al. Synergistic effect of organic plasticizer and lepidolite filler on polymer electrolytes for all-solid high-voltage Li–metal batteries. J Mater Chem A, 2020, 8, 5968
[8] Jiang C, Gu Y M, Tang M, et al. Toward stable lithium plating/stripping by successive desolvation and exclusive transport of Li ions. ACS Appl Mater Interfaces, 2020, 12, 10461
[9] Liu Y Y, Lin D C, Yuen P Y, et al. An artificial solid electrolyte interphase with high Li-ion conductivity, mechanical strength, and flexibility for stable lithium metal anodes. Adv Mater, 2017, 29, 1605531
[10] Zhang X Q, Cheng X B, Chen X, et al. Fluoroethylene carbonate additives to render uniform Li deposits in lithium metal batteries. Adv Funct Mater, 2017, 27, 1605989
[11] Li Q, Zhu S P, Lu Y Y. 3D porous Cu current collector/Li-metal composite anode for stable lithium-metal batteries. Adv Funct Mater, 2017, 27, 1606422
[12] Zhao Z M, Zhao J W, Hu Z L, et al. Long-life and deeply rechargeable aqueous Zn anodes enabled by a multifunctional brightener-inspired interphase. Energy Environ Sci, 2019, 12, 1938
[13] Zeng Y X, Zhang X Y, Qin R F, et al. Dendrite-free zinc deposition induced by multifunctional CNT frameworks for stable flexible Zn-ion batteries. Adv Mater, 2019, 31, 1903675
[14] Naveed A, Yang H J, Yang J, et al. Highly reversible and rechargeable safe Zn batteries based on a triethyl phosphate electrolyte. Angew Chem Int Ed, 2019, 58, 2760
[15] Konarov A, Voronina N, Jo J H, et al. Present and future perspective on electrode materials for rechargeable zinc-ion batteries. ACS Energy Lett, 2018, 3, 2620
[16] Chen L N, An Q Y, Mai L Q. Recent advances and prospects of cathode materials for rechargeable aqueous zinc-ion batteries. Adv Mater Interfaces, 2019, 6, 1900387
[17] Cui J, Guo Z W, Yi J, et al. Organic cathode materials for rechargeable zinc batteries: Mechanisms, challenges, and perspectives. ChemSusChem, 2020, 13, 2160
[18] Yang D, Tan H T, Rui X H, et al. Electrode materials for rechargeable zinc-ion and zinc-air batteries: Current status and future perspectives. Electrochem Energy Rev, 2019, 2, 395
[19] Selvakumaran D, Pan A Q, Liang S Q, et al. A review on recent developments and challenges of cathode materials for rechargeable aqueous Zn-ion batteries. J Mater Chem A, 2019, 7, 18209
[20] Chao D L, Zhou W H, Ye C, et al. An electrolytic Zn-MnO_2 battery for high-voltage and scalable energy storage. Angew Chem Int Ed, 2019, 58, 7823
[21] Pan H, Shao Y, Yan P, et al. Reversible aqueous zinc/manganese oxide energy storage from conversion reactions. Nat Energy, 2016, 1, 16039
[22] Li Z L, Ganapathy S, Xu Y L, et al. Mechanistic insight into the electrochemical performance of Zn/VO_2 batteries with an aqueous $ZnSO_4$ electrolyte. Adv Energy Mater, 2019, 9, 1900237
[23] Wan F, Niu Z Q. Design strategies for vanadium-based aqueous zinc-ion batteries. Angew Chem Int Ed, 2019, 58, 16358
[24] Zhang L Y, Chen L, Zhou X F, et al. Towards high-voltage aqueous metal-ion batteries beyond 1.5 V: The zinc/zinc hexacyanoferrate system. Adv Energy Mater, 2015, 5, 1400930
[25] Trócoli R, La Mantia F. An aqueous zinc-ion battery based on copper hexacyanoferrate. ChemSusChem, 2015, 8, 481
[26] Huang J H, Wang Z, Hou M Y, et al. Polyaniline-intercalated manganese dioxide nanolayers as a high-performance cathode material for an aqueous zinc-ion battery. Nat Commun, 2018, 9, 2906
[27] Lee B, Lee H R, Kim H, et al. Elucidating the intercalation mechanism of zinc ions into α-MnO_2 for rechargeable zinc batteries. Chem Commun, 2015, 51, 9265
[28] Wang C, Ren X C, Xu C H, et al. N-type 2D organic single crystals for high-performance organic field-effect transistors and near-infrared phototransistors. Adv Mater, 2018, 30, 1706260
[29] Wang Q Q, Yang F X, Zhang Y, et al. Space-confined strategy toward large-area two-dimensional single crystals of molecular materials. J Am Chem Soc, 2018, 140, 5339
[30] Lu Y, Chen J. Prospects of organic electrode materials for practical lithium batteries. Nat Rev Chem, 2020, 4, 127
[31] Tang M, Jiang C, Liu S Y, et al. Small amount COFs enhancing storage of large anions. Energy Storage Mater, 2020, 27, 35
[32] Wu Y W, Zeng R H, Nan J M, et al. Quinone electrode materials

for rechargeable lithium/sodium ion batteries. Adv Energy Mater, 2017, 7, 1700278
[33] Wang Y R, Wang C X, Ni Z G, et al. Binding zinc ions by carboxyl groups from adjacent molecules toward long-life aqueous zinc-organic batteries. Adv Mater, 2020, 32, 2000338
[34] Zhao Q, Huang W W, Luo Z Q, et al. High-capacity aqueous zinc batteries using sustainable quinone electrodes. Sci Adv, 2018, 4, eaao1761
[35] Guo Z W, Ma Y Y, Dong X L, et al. An environmentally friendly and flexible aqueous zinc battery using an organic cathode. Angew Chem Int Ed, 2018, 57, 11737
[36] Dawut G, Lu Y, Miao L C, et al. High-performance rechargeable aqueous Zn-ion batteries with a poly(benzoquinonyl sulfide) cathode. Inorg Chem Front, 2018, 5, 1391
[37] Yue X J, Liu H D, Liu P. Polymer grafted on carbon nanotubes as a flexible cathode for aqueous zinc ion batteries. Chem Commun, 2019, 55, 1647
[38] Zhang S Q, Zhao W T, Li H, et al. Cross-conjugated polycatechol organic cathode for aqueous zinc-ion storage. ChemSusChem, 2020, 13, 188
[39] Wang C L, Jiang C, Xu Y, et al. A selectively permeable membrane for enhancing cyclability of organic sodium-ion batteries. Adv Mater, 2016, 28, 9182
[40] Tang M, Zhu S L, Liu Z T, et al. Tailoring π-conjugated systems: From π-π stacking to high-rate-performance organic cathodes. Chem, 2018, 4, 2600
[41] Zhu S L, Tang M, Wu Y C, et al. Free-standing protective films for enhancing the cyclability of organic batteries. Sustain Energy Fuels, 2019, 3, 142
[42] Chen Y, Tang M, Wu Y C, et al. A one-dimensional π-d conjugated coordination polymer for sodium storage with catalytic activity in Negishi coupling. Angew Chem Int Ed, 2019, 58, 14731
[43] Li H Y, Tang M, Wu Y C, et al. Large π-conjugated porous frameworks as cathodes for sodium-ion batteries. J Phys Chem Lett, 2018, 9, 3205
[44] Wang C L, Dong H L, Hu W P, et al. Semiconducting π-conjugated systems in field-effect transistors: A material odyssey of organic electronics. Chem Rev, 2012, 112, 2208
[45] Wang C L, Dong H L, Jiang L, et al. Organic semiconductor crystals. Chem Soc Rev, 2018, 47, 422
[46] Khayum M A, Ghosh M, Vijayakumar V, et al. Zinc ion interactions in a two-dimensional covalent organic framework based aqueous zinc ion battery. Chem Sci, 2019, 10, 8889
[47] Wang C L. Weak intermolecular interactions for strengthening organic batteries. Energy Environ Mater, 2020
[48] Chen Y, Li H Y, Tang M, et al. Capacitive conjugated ladder polymers for fast-charge and -discharge sodium-ion batteries and hybrid supercapacitors. J Mater Chem A, 2019, 7, 20891
[49] Wang C L, Xu Y, Fang Y G, et al. Extended π-conjugated system for fast-charge and -discharge sodium-ion batteries. J Am Chem Soc, 2015, 137, 3124
[50] Li Z L, Zhao H L. Recent developments of phosphorus-based anodes for sodium ion batteries. J Mater Chem A, 2018, 6, 24013
[51] Kundu D P, Oberholzer P, Glaros C, et al. Organic cathode for aqueous Zn-ion batteries: Taming a unique phase evolution toward stable electrochemical cycling. Chem Mater, 2018, 30, 3874
[52] Tang M, Wu Y C, Chen Y, et al. An organic cathode with high capacities for fast-charge potassium-ion batteries. J Mater Chem A, 2019, 7, 486
[53] Nam K W, Kim H, Beldjoudi Y, et al. Redox-active phenanthrenequinone triangles in aqueous rechargeable zinc batteries. J Am Chem Soc, 2020, 142, 2541
[54] Wang N, Dong X L, Wang B L, et al. Zinc-organic battery with a wide operation-temperature window from −70 to 150 °C. Angew Chem Int Ed, 2020, 132, 14685
[55] Sun W, Wang F, Hou S, et al. Zn/MnO_2 battery chemistry with H^+ and Zn^{2+} coinsertion. J Am Chem Soc, 2017, 139, 9775
[56] Shea J J, Luo C. Organic electrode materials for metal ion batteries. ACS Appl Mater Interfaces, 2020, 12, 5361
[57] Chen Y, Zhuo S M, Li Z Y, et al. Redox polymers for rechargeable metal-ion batteries. EnergyChem, 2020, 2, 100030
[58] Ghanbari K, Mousavi M F, Shamsipur M. Preparation of polyaniline nanofibers and their use as a cathode of aqueous rechargeable batteries. Electrochim Acta, 2006, 52, 1514
[59] Somasiri N L D, MacDiarmid A G. Polyaniline: characterization as a cathode active material in rechargeable batteries in aqueous electrolytes. J Appl Electrochem, 1988, 18, 92
[60] Yamamoto K, Yamada M, Nishiumi T. Doping reaction of redox-active dopants into polyaniline. Polym Adv Technol, 2000, 11, 710
[61] Gospodinova N, Terlemezyan L. Conducting polymers prepared by oxidative polymerization: Polyaniline. Prog Polym Sci, 1998, 23, 1443
[62] Jiménez P, Levillain E, Alévêque O, et al. Lithium n-doped polyaniline as a high-performance electroactive material for rechargeable batteries. Angew Chem, 2017, 129, 1575
[63] Karyakin A A, Strakhova A K, Yatsimirsky A K. Self-doped polyanilines electrochemically active in neutral and basic aqueous solutions: Electropolymerization of substituted anilines. J Electroan Chem, 1994, 371, 259
[64] Rahmanifar M S, Mousavi M F, Shamsipur M. Effect of self-doped polyaniline on performance of secondary Zn-polyaniline battery. J Power Sources, 2002, 110, 229
[65] Shi H Y, Ye Y J, Liu K, et al. A long-cycle-life self-doped polyaniline cathode for rechargeable aqueous zinc batteries. Angew Chem Int Ed, 2018, 57, 16359
[66] Mu S L, Shi Q F. Controllable preparation of poly(aniline-co-5-aminosalicylic acid) nanowires for rechargeable batteries. Synth Met, 2016, 221, 8
[67] Mu S L. Rechargeable batteries based on poly(aniline-co-o-aminophenol) and the protonation of the copolymer. Synth Met, 2004, 143, 269
[68] Zhang J, Shan D, Mu S L. A rechargeable Zn- poly(aniline-co-m-aminophenol) battery. J Power Sources, 2006, 161, 685
[69] Chen C X, Hong X Z, Xu T T, et al. Electrosynthesis and electrochemical and electrochromic properties of poly(aniline-co-N-methylthionine). J Electrochem Soc, 2015, 162, G54
[70] Chen C X, Hong X Z, Chen A K, et al. Electrochemical properties of poly(aniline-co-N-methylthionine) for zinc-conducting polymer rechargeable batteries. Electrochim Acta, 2016, 190, 240
[71] Chen C X, Gan Z Y, Xu C, et al. Electrosynthesis of poly(aniline-co-azure B) for aqueous rechargeable zinc-conducting polymer batteries. Electrochim Acta, 2017, 252, 226
[72] Liu Y, Xie L Y, Zhang W, et al. A conjugated system of PEDOT: PSS induced self-doped PANI for flexible zinc-ion batteries with enhanced capacity and cyclability. ACS Appl Mater Interfaces, 2019, 11, 30943
[73] Wang Z, Han J J, Zhang N, et al. Synthesis of polyaniline/graphene composite and its application in zinc-rechargeable batteries. J Solid State Electrochem, 2019, 23, 3373
[74] Du W C, Xiao J F, Geng H B, et al. Rational-design of polyaniline cathode using proton doping strategy by graphene oxide for enhanced aqueous zinc-ion batteries. J Power Sources, 2020, 450, 227716
[75] Yao H, Li Q J, Zhang M S, et al. Prolonging the cycle life of zinc-ion battery by introduction of $[Fe(CN)_6]^{4-}$ to PANI via a simple and scalable synthetic method. Chem Eng J, 2020, 392, 123653
[76] Li P, Fang Z S, Zhang Y, et al. A high-performance, highly bendable quasi-solid-state zinc–organic battery enabled by intelligent proton-self-buffering copolymer cathodes. J Mater Chem A, 2019, 7, 17292

[77] Trinidad F. Performance study of Zn/$ZnCl_2$,NH_4Cl/polyaniline/carbon battery. J Electrochem Soc, 1991, 138, 3186
[78] Ghanbari K, Mousavi M F, Shamsipur M, et al. Synthesis of polyaniline/graphite composite as a cathode of Zn-polyaniline rechargeable battery. J Power Sources, 2007, 170, 513
[79] Xia Y, Zhu D R, Si S H, et al. Nickel foam-supported polyaniline cathode prepared with electrophoresis for improvement of rechargeable Zn battery performance. J Power Sources, 2015, 283, 125
[80] Wan F, Zhang L L, Wang X Y, et al. An aqueous rechargeable zinc-organic battery with hybrid mechanism. Adv Funct Mater, 2018, 28, 1804975
[81] Yu H, Liu G, Wang M, et al. Plasma-assisted surface modification on the electrode interface for flexible fiber-shaped Zn–polyaniline batteries. ACS Appl Mater Interfaces, 2020, 12, 5820
[82] Xiao X C, Liu W J, Wang K, et al. High-performance solid-state Zn batteries based on a free-standing organic cathode and metal Zn anode with an ordered nano-architecture. Nanoscale Adv, 2020, 2, 296
[83] Cao H M, Wan F, Zhang L L, et al. Highly compressible zinc-ion batteries with stable performance. J Mater Chem A, 2019, 7, 11734
[84] Zhang Y, Wang Q R, Bi S S, et al. Flexible all-in-one zinc-ion batteries. Nanoscale, 2019, 11, 17630
[85] Huang S, Wan F, Bi S S, et al. A self-healing integrated all-in-one zinc-ion battery. Angew Chem, 2019, 131, 4357
[86] Bi S S, Wan F, Huang S, et al. A flexible quasi-solid-state bifunctional device with zinc-ion microbattery and photodetector. ChemElectroChem, 2019, 6, 3933
[87] Zhao Y, Wang Y N, Zhao Z M, et al. Achieving high capacity and long life of aqueous rechargeable zinc battery by using nanoporous-carbon-supported poly(1, 5-naphthalenediamine) nanorods as cathode. Energy Storage Mater, 2020, 28, 64
[88] Wang J Q, Liu J, Hu M M, et al. A flexible, electrochromic, rechargeable Zn//PPy battery with a short circuit chromatic warning function. J Mater Chem A, 2018, 6, 11113
[89] Li Z X, Huang Y, Zhang J Y, et al. One-step synthesis of MnO_x/PPy nanocomposite as a high-performance cathode for a rechargeable zinc-ion battery and insight into its energy storage mechanism. Nanoscale, 2020, 12, 4150
[90] Li X W, Xie X L, Lv R, et al. Nanostructured polypyrrole composite aerogels for a rechargeable flexible aqueous Zn-ion battery with high rate capabilities. Energy Technol, 2019, 7, 1801092
[91] Li S, Sultana I, Guo Z P, et al. Polypyrrole as cathode materials for Zn-polymer battery with various biocompatible aqueous electrolytes. Electrochim Acta, 2013, 95, 212
[92] Lahiri A, Yang L, Li G Z, et al. Mechanism of Zn-ion intercalation/deintercalation in a Zn-polypyrrole secondary battery in aqueous and bio-ionic liquid electrolytes. ACS Appl Mater Interfaces, 2019, 11, 45098
[93] Grgur B N, Gvozdenović M M, Stevanović J, et al. Polypyrrole as possible electrode materials for the aqueous-based rechargeable zinc batteries. Electrochim Acta, 2008, 53, 4627
[94] Cxiricx-Marjanovicx G, Mentus S. Charge-discharge characteristics of polythiopheneas a cathode active material in a rechargeable battery. J Appl Electrochem, 1998, 28, 103
[95] Simons T J, Salsamendi M, Howlett P C, et al. Rechargeable Zn/PEDOT battery with an imidazolium-based ionic liquid as the electrolyte. ChemElectroChem, 2015, 2, 2071
[96] Fdz de Anastro A, Casado N, Wang X E, et al. Poly(ionic liquid) iongels for all-solid rechargeable zinc/PEDOT batteries. Electrochim Acta, 2018, 278, 271
[97] Pandey P C. Electrochemical synthesis of polyindole and its evaluation for rechargeable battery applications. J Electrochem Soc, 1998, 145, 999
[98] Cai Z J, Hou C W. Study on the electrochemical properties of zinc/polyindole secondary battery. J Power Sources, 2011, 196, 10731
[99] Liu Z, Prowald A, Höfft O, et al. An ionic liquid-surface functionalized polystyrene spheres hybrid electrolyte for rechargeable zinc/conductive polymer batteries. ChemElectroChem, 2018, 5, 2321
[100] Cai Z J, Guo J, Yang H Z, et al. Electrochemical properties of electrospun poly(5-cyanoindole) submicron-fibrous electrode for zinc/polymer secondary battery. J Power Sources, 2015, 279, 114
[101] Nigrey P J. Lightweight rechargeable storage batteries using polyacetylene, $(CH)_x$ as the cathode-active material. J Electrochem Soc, 1981, 128, 1651
[102] Häupler B, Rössel C, Schwenke A M, et al. Aqueous zinc-organic polymer battery with a high rate performance and long lifetime. NPG Asia Mater, 2016, 8, e283
[103] Wang X S, Chen L, Lu F, et al. Boosting aqueous Zn^{2+} storage in 1, 4, 5, 8-naphthalenetetracarboxylic dianhydride through nitrogen substitution. ChemElectroChem, 2019, 6, 3644
[104] Peng C, Ning G H, Su J, et al. Reversible multi-electron redox chemistry of π-conjugated N-containing heteroaromatic molecule-based organic cathodes. Nat Energy, 2017, 2, 17074
[105] Kapaev R R, Zhidkov I S, Kurmaev E Z, et al. Hexaazatriphenylene-based polymer cathode for fast and stable lithium-, sodium- and potassium-ion batteries. J Mater Chem A, 2019, 7, 22596
[106] Tie Z W, Liu L J, Deng S Z, et al. Proton insertion chemistry of a zinc-organic battery. Angew Chem Int Ed, 2020, 59, 4920
[107] Cheng L W, Liang Y H, Zhu Q N, et al. Bio-inspired isoalloxazine redox moieties for rechargeable aqueous zinc-ion batteries. Chem - Asian J, 2020, 15, 1290
[108] Glatz H, Lizundia E, Pacifico F, et al. An organic cathode based dual-ion aqueous zinc battery enabled by a cellulose membrane. ACS Appl Energy Mater, 2019, 2, 1288
[109] Koshika K, Sano N, Oyaizu K, et al. An aqueous, electrolyte-type, rechargeable device utilizing a hydrophilic radical polymer-cathode. Macromol Chem Phys, 2009, 210, 1989
[110] Luo Y W, Zheng F P, Liu L J, et al. A high-power aqueous zinc-organic radical battery with tunable operating voltage triggered by selected anions. ChemSusChem, 2020, 13, 2239
[111] Jiang C, Tang M, Zhu S L, et al. Constructing universal ionic sieves via alignment of two-dimensional covalent organic frameworks (COFs). Angew Chem Int Ed, 2018, 57, 16072
[112] Jiang C, Wang C L. 2D materials as ionic sieves for inhibiting the shuttle effect in batteries. Chem - Asian J, 2020, 15, 2294
[113] Yan L J, Zhao C X, Sha Y, et al. Electrochemical redox behavior of organic quinone compounds in aqueous metal ion electrolytes. Nano Energy, 2020, 73, 104766
[114] Yan L J, Zeng X M, Li Z H, et al. An innovation: Dendrite free quinone paired with $ZnMn_2O_4$ for zinc ion storage. Mater Today Energy, 2019, 13, 323
[115] Guerfi A, Trottier J, Boyano I, et al. High cycling stability of zinc-anode/conducting polymer rechargeable battery with non-aqueous electrolyte. J Power Sources, 2014, 248, 1099
[116] Kitani A. Performance study of aqueous polyaniline batteries. J Electrochem Soc, 1986, 133, 1069
[117] Liu P F, Lv R, He Y, et al. An integrated, flexible aqueous Zn-ion battery with high energy and power densities. J Power Sources, 2019, 410/411, 137
[118] Shan D, Mu S L. Electrochemical characteristics of polyaniline synthesized in the presence of ferrocenesulfonic acid. Synth Met, 2002, 126, 225
[119] Karami H, Mousavi M F, Shamsipur M. A new design for dry polyaniline rechargeable batteries. J Power Sources, 2003, 117, 255